DOI: 10.1002/cmdc.200800422

Cyclic RGD-Containing Functionalized Azabicycloalkane Peptides as Potent Integrin Antagonists for Tumor Targeting

Leonardo Manzoni,*[a] Laura Belvisi,*[b, c] Daniela Arosio,[a] Monica Civera,[c] Michael Pilkington-Miksa,[c] Donatella Potenza,[b, c] Andrea Caprini,[c] Elena M. V. Araldi,[c] Eugenia Monferini,[c] Monica Mancino,[d] Francesca Podestà,[d] and Carlo Scolastico[b, c]

Cyclic RGD-containing functionalized azabicycloalkane peptides were synthesized with the aim of developing high-affinity selective integrin ligands as carriers for therapeutic and diagnostic purposes. Herein we describe the synthesis and in vitro screening of these RGD derivatives, as well as the determination of their conformational properties in solution by spectroscopic and computational methods. Docking studies with the X-ray crystal structure of the extracellular domain of integrin $\alpha_v\beta_3$ were also performed to elucidate the structural binding requirements and to rationalize the biological results. One compound in particular was found to be the best $\alpha_v\beta_3$ integrin binder ($IC_{50} = 53.7$ nM) among the new functionalized RGD cyclic peptides, thus emerging as a promising candidate for covalent bonding and selective homing of useful functional units.

Introduction

Tumors produce many angiogenic factors that are able to activate endothelial cells in established blood vessels and induce endothelial proliferation, migration, and new vessel formation. Angiogenesis is a requirement for both tumor growth and metastasis.[1] The angiogenic process depends mainly on vascular endothelial cell migration, which is regulated by cell adhesion receptors. Integrins are transmembrane-spanning receptors that participate in cell-matrix interactions in all normal and malignant cell types.[2] The most common integrins recognize the tripeptide sequence Arg-Gly-Asp (RGD), found in many extracellular matrix adhesive proteins.[3] The context of the RGD sequence (flanking residues, 3D presentation, and individual features of the integrin binding pockets) determines the specificity and efficacy of interaction.[4] It is therefore a major challenge to identify compounds that can discriminate between RGD-binding integrins implicated in human pathologies. Thus, the vitronectin receptors $\alpha_v\beta_3$ and $\alpha_v\beta_5$ emerged as potential therapeutic targets for the treatment of osteoporosis, restenosis, ocular disease, tumor-induced angiogenesis, metastasis formation, and sickle-cell anemia.[5]

Endothelial cells in the angiogenic vessels within solid tumors express several proteins that are absent or hardly detectable in established blood vessels, including integrins and receptors for certain angiogenic growth factors. The $\alpha_v\beta_3$ integrin, for instance, is expressed at low levels on epithelial cells and mature endothelial cells; however, it is highly expressed on activated endothelial cells in the neovasculature of tumors, including osteosarcomas, neuroblastomas, glioblastomas, melanomas, lung carcinomas, and breast cancer. Furthermore, antagonists of $\alpha_v\beta_3$ integrins significantly inhibit vessel development and tumor growth induced by cytokines and solid tumor fragments.[6] Notably, $\alpha_v\beta_3$ antagonists have very little effect on preexisting blood vessels, indicating the usefulness of targeting this receptor for therapeutic benefit without adverse side effects. Besides the $\alpha_v\beta_3$ integrin, the $\alpha_v\beta_5$ integrin has also been implicated in the angiogenic process, possibly via a signaling pathway distinct from that of $\alpha_v\beta_3$.[7] Therefore, selective antagonists of $\alpha_v\beta_3$ and/or $\alpha_v\beta_5$ may be useful in blocking tumor-induced angiogenesis.

A few years ago the crystal structure of the extracellular segment of integrin $\alpha_v\beta_3$ complexed with the cyclic pentapeptide ligand *cyclo*-(Arg-Gly-Asp-D-Phe-[*N*-Me]Val) (EMD121974) was reported.[8] The crystal structure of the peptide–integrin complex provides the exact conformation of EMD121974 bound to $\alpha_v\beta_3$ integrin, and serves as a basis for understanding the gen-

[a] *Dr. L. Manzoni, Dr. D. Arosio*
Istituto di Scienze e Tecnologie Molecolari
Consiglio Nazionale delle Ricerche
Via Fantoli 16/15, 20138 Milano (Italy)
Fax: (+39) 02 50320945
E-mail: leonardo.manzoni@istm.cnr.it

[b] *Dr. L. Belvisi, Dr. D. Potenza, Prof. C. Scolastico*
Dipartimento di Chimica Organica e Industriale
Università degli Studi di Milano
Via Venezian 21, 20133 Milano (Italy)
Fax: (+39) 02 50314072
E-mail: laura.belvisi@unimi.it

[c] *Dr. L. Belvisi, Dr. M. Civera, Dr. M. Pilkington-Miksa, Dr. D. Potenza, Dr. A. Caprini, E. M. V. Araldi, E. Monferini, Prof. C. Scolastico*
Centro Interdisciplinare Studi biomolecolari e applicazioni Industriali
Università degli Studi di Milano
Via Fantoli 16/15, 20138 Milano (Italy)

[d] *Dr. M. Mancino, Dr. F. Podestà*
IRCCS Multimedica, Via Fantoli 16/15, 20138 Milano (Italy)

Supporting information for this article is available on the WWW under http://dx.doi.org/10.1002/cmdc.200800422.

eral mode of interaction of integrins with other RGD-containing ligands.

Cyclic RGD peptides have been developed by various research groups as active and selective integrin antagonists that compete with matrix molecules for specific integrin receptors.[9] The conformational constraint imposed by the cyclic template has been shown to be a valuable tool in the indirect determination of the bioactive conformation. The pioneering work in this field by Kessler and co-workers has led to a highly active $\alpha_v\beta_3$-selective first-generation cyclic pentapeptide: *cyclo*-(Arg-Gly-Asp-D-Phe-Val).[10] Extensive modification of this lead structure with various peptidomimetics and carbohydrate scaffolds has been performed, and new potent antagonists have been identified.[11] Systematic derivatization of the lead peptide resulted in the N-alkylated cyclopeptide mentioned above, *cyclo*-(Arg-Gly-Asp-D-Phe-[*N*-Me]Val) (EMD121974), which has entered clinical phase II studies as an angiogenesis inhibitor.[12,13]

Among the conformationally constrained cyclic RGD peptides discovered over the last decade as $\alpha_v\beta_3/\alpha_v\beta_5$ binders with affinity in the low-nanomolar range, is notably a series of cyclic tetrapeptide ligands containing γ-aminocyclopentanecarboxylic acid fragments or 4-aminoproline residues.[14a,b] In particular, the use of the γ-amino and carboxyl functions of the 4-aminoproline scaffold to generate 14-membered RGD cyclotetrapeptides resulted in the discovery of sub-nanomolar $\alpha_v\beta_3/\alpha_v\beta_5$ ligands, leaving the Nα-proline site free for conjugation to useful functional units.

In this context, our research group has reported a library of 15-membered cyclic RGD pentapeptide mimics based on 1-aza-2-oxobicyclo[X.3.0]alkane amino acids.[15] Stereoisomeric 6,5- and 7,5-fused bicyclic lactams **1** with different reverse-turn mimetic properties were exploited as dipeptide analogues for the synthesis of a library of the general formula *cyclo*-(Arg-Gly-Asp-lactam) **2** (Figure 1). The replacement of the D-Phe-Val dipeptide in the lead structure *cyclo*-(RGDfV) with such azabicycloalkane scaffolds showing different reverse-turn mimetic properties constrains the RGD sequences into different conformations and provides the required activity and selectivity for integrin antagonism. This library was found to contain specific high-affinity ligands for $\alpha_v\beta_3$ and $\alpha_v\beta_5$ integrins, which are presently under evaluation as very promising anti-angiogenic drugs. Among the peptides tested, **3** (ST1646) showed the highest affinity for $\alpha_v\beta_3$ and $\alpha_v\beta_5$, inhibiting echistatin binding to $\alpha_v\beta_3$ and $\alpha_v\beta_5$ with IC_{50} values of 3.7 ± 0.6 and 1.39 ± 0.2 nM, respectively (Figure 1).[16]

The functionalization of such azabicycloalkane scaffolds with heteroalkyl substituents is of great interest, as it allows the conjugation of various chemical entities for application in medical diagnosis and therapeutics. New research in the integrin field suggests that high-affinity integrin ligands can express their potential not only as such, but even as intelligent vectors for other active units. The RGD ligand– active unit conjugates may be selectively targeted to those tissues that overexpress integrins (such as epithelial cells involved in vascular growth) and selectively control the release of a drug (i.e. a cytotoxic agent) bound to the lactam ring as well as inhibit angiogenesis. Furthermore, the targeting of biological pathways with molecular imaging probes holds great promise as a means of detecting and diagnosing disease at a much earlier stage than is the norm today. The low number of "scaffolds" suitable for the preparation of conjugated integrin ligands and the necessity to obtain them in high yield over a minimal number of steps, forced us to design and synthesize novel conformationally constrained dipeptide mimetics, functionalized with hetero-substituted side chains.[14,17,18]

Herein we report the synthesis, conformational analysis by spectroscopic and computational methods, in vitro evaluation toward $\alpha_v\beta_3$ and $\alpha_v\beta_5$ integrins, and docking studies of cyclic RGD compounds (**5**, Figure 1) containing the conformationally constrained homoSer-Pro dipeptide unit structure (**4**, Figure 1). These compounds could be useful as anti-angiogenic drugs; moreover, they are particularly suitable candidates as vectors for therapeutics and diagnostics.

Results and Discussion

Chemistry

The synthesis of compounds of general formula **5**, shown in Figure 1, required the preparation of scaffolds **6**–**9** (Figure 2). These were obtained through a known synthetic procedure based on a stereoselective 1,3-dipolar nitrone cycloaddition on suitably protected allylprolines.[18] With these precursors in hand, we started the synthesis of the cyclic RGD compounds.

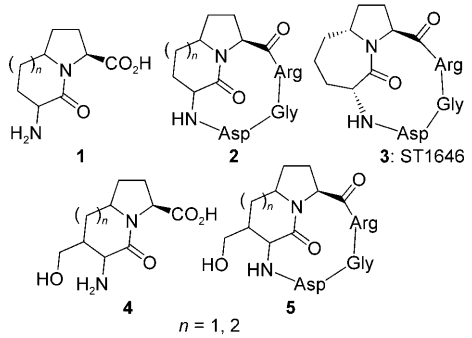

Figure 1. Integrin ligands and scaffolds used in their preparation.

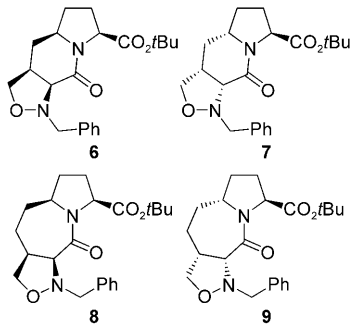

Figure 2. Bicyclic lactam templates **6**–**9**.

The synthetic plan for preparation of the RGD pseudopeptides was based on a linear peptide synthesis in solution using the benzyloxycarbonyl (Cbz) protection strategy, followed by cyclization and side chain deprotection. To minimize steric hindrance at the cyclization site and to avoid the possibility of C-terminal racemization, cyclization between the Gly and Asp residues was envisaged, and the linear peptides **10**–**13** were chosen as the target linear sequences (Figure 3). Arg and Asp,

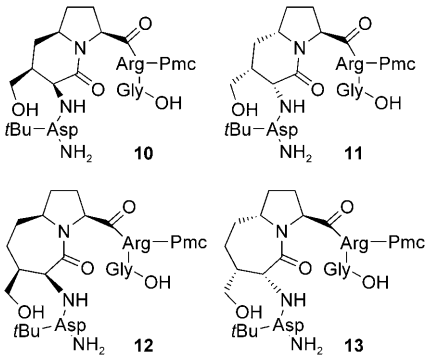

Figure 3. Linear pseudopeptides H_2N-Asp(*t*Bu)-Temp-Arg(Pmc)-Gly-OH **10**–**13**; Temp = azabicycloalkane scaffold.

with the side chains protected using 2,2,5,7,8-pentamethylchroman-6-sulfonyl (Pmc) and *tert*-butyl groups, respectively, were employed in the synthesis. Both these protecting groups are removed under acidic conditions, and are therefore compatible with the Cbz strategy.

The first step in the synthesis consisted of the deprotection of the *tert*-butyl ester of the bicyclic lactams **6**–**9** by treatment with trifluoroacetic acid (TFA) in dichloromethane to give the corresponding carboxylic acids in quantitative yields (Scheme 1). These compounds were used in the subsequent coupling step without further purification.

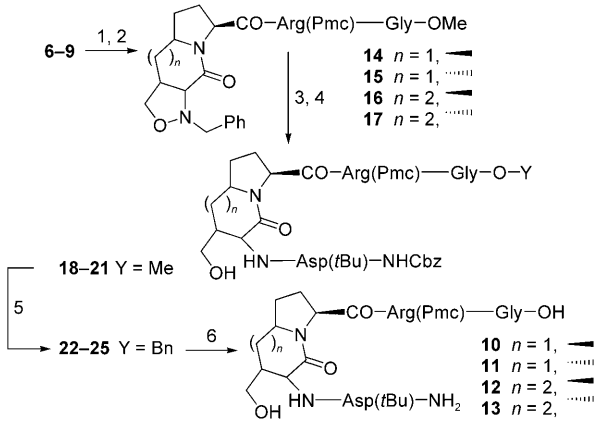

Scheme 1. Synthesis of the protected linear peptides **10**–**13**. Reagents and conditions: 1) TFA, CH_2Cl_2; 2) H-Arg(Pmc)-Gly-OMe, DIC, HOBt, THF/CH_2Cl_2, 30–90% over two steps; 3) H_2, Pd/C, MeOH, 5 atm, 3 days; 4) DIC, HOBt, TEA, Z-Asp(*t*Bu)-OH, THF, −30 °C, 60–87% over two steps; 5) BnOH, Ti(*i*PrO)$_4$, THF, 90 °C, 67–90%; 6) H_2, Pd/C, MeOH.

The dipeptide H-Arg(Pmc)-Gly-OMe was coupled to the free carboxyl group of bicyclic lactams **6**–**9** using 1,3-diisopropylcarbodiimide (DIC)/1-hydroxy-1*H*-benzotriazole (HOBt) to furnish the desired products **15** and **17** in good yields, whereas for compounds **14** and **16**, the yields were lower (Scheme 1).[19]

After conversion of the *N*-benzyloxazolidine function of compounds **14**–**17** into the appropriate amino alcohols by hydrogenation on Pd/C at 5 atm, Cbz-Asp(O*t*Bu)-OH was coupled to the free amine. The reaction was performed by using an equimolar ratio of Cbz-Asp(O*t*Bu)-OH and free amine at −30 °C in order to avoid the undesired condensation of the amino acid with the free hydroxy group of the scaffold. The low yield observed in the methyl ester hydrolysis of compounds **18**–**21** under standard, basic conditions forced us to change the glycine carboxylic acid protecting group. Acid-catalyzed transesterification mediated by Ti(O*i*Pr)$_4$ in the presence of excess benzyl alcohol gave **22**–**25** with two simultaneously removable protecting groups. Hydrogenation on Pd/C followed by cyclization using *O*-(7-azabenzotriazol-1-yl)-*N*,*N*,*N*′,*N*′-tetramethyluronium hexafluorophosphate (HATU) and 7-aza-1-hydroxy-1*H*-benzotriazole (HOAt) as condensing agents provided protected cyclic pseudopentapeptides **26**–**29** in 54–74% yield over two steps (Scheme 2).

Finally, the side chain protecting groups of compounds **26**–**29** were removed by TFA in the presence of cation scavengers. Compounds **30**, **31**, and **33** were obtained in good yields (85–98%) after HPLC purification, unlike compound **32**, which was recovered in only 30% yield. The low yield was due to the formation of many byproducts during the deprotection reaction, the most relevant of which appeared to be the product obtained from the shift of the aspartic acid residue from the amine to the hydroxy group of the side chain.[20]

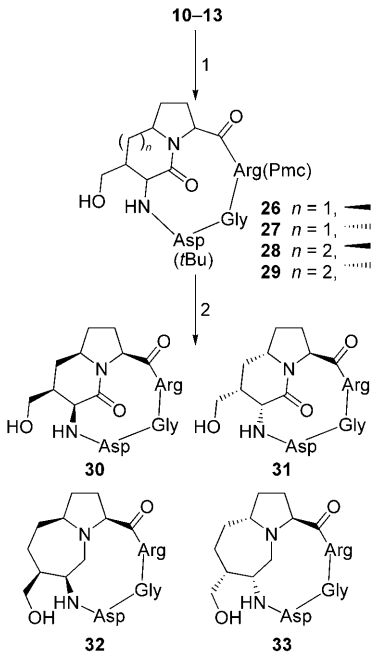

Scheme 2. Cyclization of **10**–**13** and deprotection. Reagents and conditions: 1) HATU, HOAt, DIPEA, DMF, 54–74%; 2) TFA/thioanisole/1,2-ethanedithiol/anisole (90:5:3:2), 85–98%.

With the aim of exploring the application of these functionalized cyclic RGD pseudopeptides in conjugation reactions and to evaluate the effect that a substituent would have on their activity, we decided to investigate the formation of an amide bond by preparing the corresponding valeroylamido derivatives. The synthesis of the amide derivatives was performed as follows: the hydroxy groups of compounds **26**–**29** were transformed into azido derivatives via mesylate displacement. The azido compounds **34**, **35**, and **37** were subjected to standard hydrogenation on Pd/C to afford the corresponding amines, which were condensed with valeroyl chloride to give the desired amides **38**–**40** (Scheme 3). The amide derivative of compound **28** was not obtained because azide **36** submitted to standard hydrogenation conditions afforded a complex mixture containing, apart from the desired product, two main impurities that were difficult to purify. No improvement was obtained by performing the reduction of azide **36** under Staudinger conditions. Given the difficulty in obtaining the corresponding amine, we decided to synthesize the ester derivative by simply reacting compound **28** with valeroyl chloride. The protecting groups of amides **38**–**40** and ester **41** were removed under the conditions reported above, and the resulting TFA salts were purified by HPLC (Scheme 3) to afford compounds **42**–**44** and **45**, respectively.

For compound **31**, which showed the best results in the binding assay as reported in Table 1, a scale-up procedure was performed (see Supporting Information). The reaction steps were improved in order to obtain better yields, shorter reaction times and, where possible, to economize reagents and solvents.

Table 1. Inhibition of biotinylated vitronectin binding to $\alpha_v\beta_3$ and $\alpha_v\beta_5$ receptors.

Compound	IC_{50} [nM][a]	
	$\alpha_v\beta_3$	$\alpha_v\beta_5$
vitronectin	47.1 ± 10.0	13.7 ± 6.2
cyclo-(RGDfV)	3.2 ± 1.3	7.5 ± 4.8
ST1646	1.0 ± 0.5	1.4 ± 0.8
30	1816 ± 612	> 10000
31	53.7 ± 17.3	205 ± 33.5
32	88 ± 7.3	929 ± 149
33	460 ± 126	334 ± 83.4
42	> 10000	> 10000
43	114 ± 59	234 ± 78
44	> 10000	> 10000
45	1850 ± 300	1527 ± 416

[a] IC_{50} values were calculated as the concentration of compound required for 50% inhibition of biotinylated vitronectin binding as estimated by GraphPad Prism software; all values are the mean ± SD of triplicate determinations.

Biological evaluation

Receptor binding assay

The cyclic pentapeptides **30**–**33**, the amide derivatives **42**–**44**, and the ester derivative **45** were examined in vitro for their ability to compete with biotinylated vitronectin for binding to the purified $\alpha_v\beta_3$ and $\alpha_v\beta_5$ receptors (Table 1). Screening assays were performed by measuring the effects of the RGD pentapeptide mimics on the interaction between immobilized integrin receptors and soluble biotinylated ligands. The ability of the new compounds to inhibit the binding of vitronectin to the isolated $\alpha_v\beta_3$ and $\alpha_v\beta_5$ receptors was compared with that of the standard compound, *cyclo*-(RGDfV), and that of compound ST1646, whose affinity for the $\alpha_v\beta_3$ and $\alpha_v\beta_5$ integrins was previously determined in competitive binding experiments using radiolabeled echistatin.[16] Among the eight new peptides tested, compound **31** showed the highest affinity toward $\alpha_v\beta_3$ and $\alpha_v\beta_5$ integrins, inhibiting the binding of biotinylated vitronectin to $\alpha_v\beta_3$ and $\alpha_v\beta_5$ with IC_{50} values of 53.7 ± 17.3 and 205 ± 33.5 nM, respectively. However, cyclopentapeptide **31** has lower affinity toward $\alpha_v\beta_3$ and $\alpha_v\beta_5$ integrins than the low-nanomolar reference ligand ST1646. Nevertheless, the nanomolar-range affinities of ligand **31** and its corresponding amide derivative **43** toward $\alpha_v\beta_3$ integrin suggest that these function-

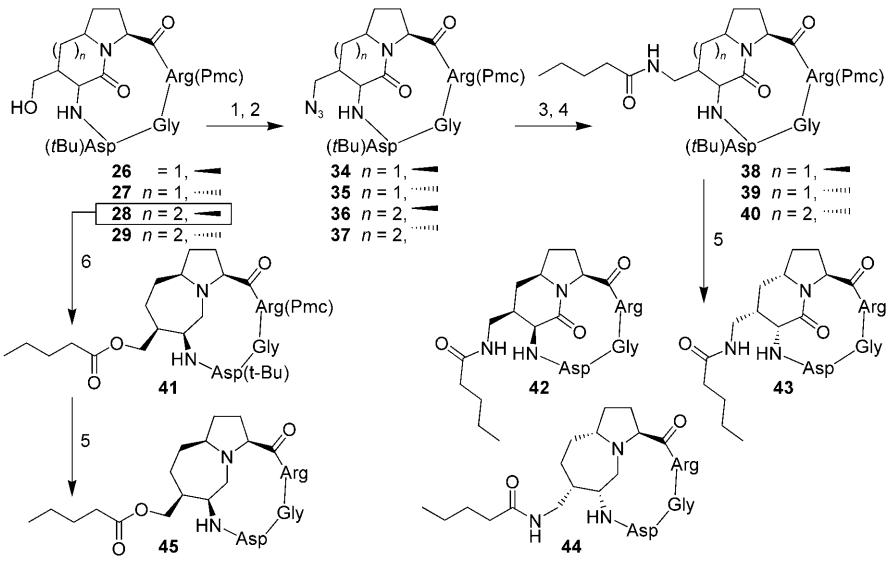

Scheme 3. Synthesis of the amide derivatives **42**–**44** and ester **45**. Reagents and conditions: 1) MsCl, TEA, CH_2Cl_2; 2) NaN_3, DMF, 80 °C, 62–90% over two steps; 3) H_2, Pd/C, MeOH; 4) valeroyl chloride, TEA, CH_2Cl_2, 40–57% over two steps; 5) TFA/thioanisole/1,2-ethanedithiol/anisole (90:5:3:2), 98%; 6) valeroyl chloride, pyridine, DMAP, THF, 84%.

alized RGD cyclic peptides could be suitable vectors for targeted drug delivery.

Cell adhesion and wound assays

To assess the activity of compound **31** as an integrin antagonist, cell adhesion assays were performed using two cell models: human umbilical vein vascular endothelial cells (HUVEC) and bladder carcinoma cells (ECV-304). Cells were allowed to adhere to immobilized fibronectin or vitronectin in the presence of increasing concentrations of the compound. An adhesion assay to uncoated plastic Petri dishes was included as a control. As shown in Table 2, compound **31** significantly inhibited cell adhesion of both cell types to either fibronectin or vitronectin in a similar micromolar range. As expected, compound **31** does not interfere with the binding to the unrelated substrate plastic.

Table 2. Effect of compound **31** on HUVEC and ECV-304 cell adhesion to plastic, fibronectin, or vitronectin.

Cell type	IC_{50} [μM][a]		
	Plastic	Fibronectin	Vitronectin
HUVEC	>100	26.2 ± 1.4	29.5 ± 1.1
ECV-304	>100	25.0 ± 1.5	14.1 ± 1.6

[a] Each data point was performed in triplicate in two independent experiments.

Fibronectin, vitronectin, and the related integrin receptors play crucial and specific roles during angiogenic events. In particular, the fibronectin–$\alpha_5\beta_1$ complex is mainly involved in developmental angiogenesis, whereas vitronectin–$\alpha_v\beta_3$ and vitronectin–$\alpha_v\beta_5$ are related mainly to postnatal tumor angiogenesis.[21] Therefore, to evaluate the suitability of compound **31** as an integrin antagonist for tumor targeting, we performed wound assay experiments on HUVEC and ECV-304 cells grown on immobilized vitronectin. As shown in Figure 4 and the Supporting Information, treatment with compound **31** at 10 μM significantly slows healing of the wounded area in the two cell types. Moreover, through Trypan blue exclusion assays, we demonstrated that compound **31** does not exert a cytotoxic effect on these two cell types; the percentage of dead cells grown on vitronectin and exposed to 10 μM compound **31** is, in fact, less than 0.1% (data not shown). Taken together, these results indicate that compound **31** acts efficiently as an $\alpha_v\beta_3$/$\alpha_v\beta_5$–integrin antagonist by interfering with both cell adhesion and movement on vitronectin, with no evidence of cytotoxic activity.

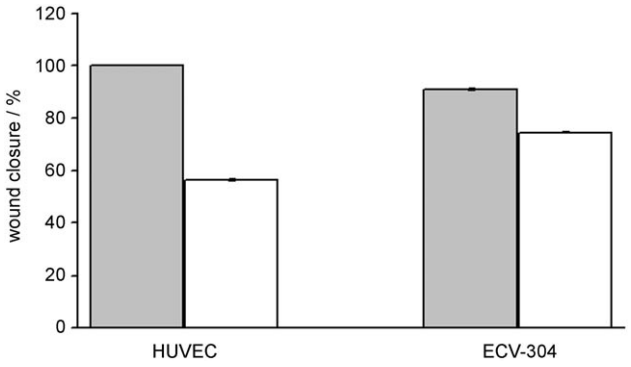

Figure 4. Compound **31** (□) at 10 μM affects wound closure on HUVEC and ECV-304 cells. The experiment was carried out in duplicate, with untreated cells (■) as reference.

Computational studies

Conformational analysis

Monte Carlo/energy minimization (MC/EM) conformational searches were performed on the *cyclo*-(Ala-Gly-Ala-lactam) pentapeptide analogues **30a**–**33a** to investigate the effects of functionalized azabicycloalkane scaffolds on the cyclopeptide conformations.[22] The principal types of backbone geometries calculated for these compounds and their relative stabilities are reported in Table 3.

As discussed previously for the library of RGD mimics **2** incorporating the unsubstituted 6,5- and 7,5-bicyclic lactams **1**,[23] depending on the lactam ring size and stereochemistry, the calculated geometries of compounds **30a**–**33a** can adopt specific secondary structure elements of peptides, in particular γ and β turns. In line with previous work,[23] the classification of the low-energy conformers of compounds **30a**–**33a** into specific β/γ turn types was based, where possible, on the ideal values of the ϕ and ψ backbone torsional angles ($\pm30^\circ$), according to the definition of Rose et al.[24]

Due to the conformational constraints introduced by the cyclic pentapeptide system and by the rigid scaffold, the peptide backbone is forced to adopt only few types of geometries. Notably, the β/γ turn arrangements reported in Table 3 for the low-energy conformers of mimics **30a**–**33a** match the four types of significant geometries already detected for the cyclic RGD pentapeptide mimics **2** and are denoted as type SI, SII, SIII, and SIV geometries (see Supporting Information).[23]

In these four types of cyclopeptide geometries, the AGA sequence adopts different kinked conformations characterized by a specific Cβ(Ala)–Cβ(Ala) distance (see Table 3). The strongest kink corresponds to the shortest Cβ–Cβ value and to the type SI geometry. In such a conformation the bicyclic unit occupies the $i+1$ and the $i+2$ positions of the βII′ turn, and the Gly residue the $i+1$ position of the γ turn. On the opposite site, the most extended conformation of the AGA sequence corresponds to the highest Cβ–Cβ distance value and to the type SIV geometry, featuring the Pro residue of the lactam ring in the $i+1$ position of the βI turn, and the Ala replacing Asp residue in the $i+1$ position of the inverse γ turn. The other two geometries featuring the SII and SIII structural types present a γ turn at Gly or an inverse γ turn at Ala (Asp), respectively, in combination with a distorted βII′ turn with Gly at the $i+1$ position, and show intermediate values of the Cβ–Cβ distance.

Monte Carlo/stochastic dynamics (MC/SD) simulations of the cyclic RGD pentapeptide mimics **30**–**33** were then performed

Table 3. Characteristics of conformers found within 3 kcal mol^{-1} of the global minimum (MC/EM, AMBER*, H_2O GB/SA) for the lactam ring CH_2OH functionalized *cyclo*-(Ala-Gly-Ala-lactam) pentapeptide mimics **30a**–**33a**.[a]

Compound	ΔE [kcal mol^{-1}]	Conformation	Cβ(Ala)–Cβ(Ala) [Å]
30a: *cyclo*-(Ala-Gly-Ala-6,5-*cis S*)	0.00	type SIV inverse γ(Asp)/βI(Pro,Arg)	9.36
	0.86	type SII γ(Gly)/βII′(Gly,Asp)[b]	8.22
	2.75	type SI γ(Gly)/βII′(lactam)	7.48
31a: *cyclo*-(Ala-Gly-Ala-6,5-*trans R*)	0.00	type SIV inverse γ(Asp)/βI(Pro,Arg)	9.39
	0.32	type SIII inverse γ(Asp)/βII′(Gly,Asp)[b]	8.62
32a: *cyclo*-(Ala-Gly-Ala-7,5-*cis S*)	0.00	type SIV inverse γ(Asp)/βI(Pro,Arg)	9.34
33a: *cyclo*-(Ala-Gly-Ala-7,5-*trans R*)	0.00	type SIII inverse γ(Asp)/βII′(Gly,Asp)[b]	8.52
	0.35	type SII γ(Gly)/βII′(Gly,Asp)[b]	8.22
	1.35	type SIV inverse γ(Asp)/βI(Pro,Arg)	9.36

[a] The lowest-energy conformer of each conformational family within 3 kcal mol^{-1} of the global minimum is described. [b] Distorted type II′ β turn.

in water,[25] as implicitly represented by the generalized Born/surface area (GB/SA) solvation model,[26] starting from the cyclopeptide backbone geometries located by the previous MC/EM step. The population of the various β/γ turn arrangements during the 10-ns MC/SD simulations for compounds **30**–**33** is reported in Table 4. For each compound, the MC/SD results closely agree with the set of MC/EM low-energy conformers of Table 3.

Compound **30** adopts the type SII geometry (γ turn at Gly and βII′ turn at Gly-Asp) characterized by a slightly kinked conformation of the RGD sequence for 57% of the simulation and the extended type SIV geometry (inverse γ turn at Asp and βI turn at Pro-Arg) for 29% of the simulation. According to the MC/EM and MC/SD results, the type SIII (inverse γ turn at Asp and βII′ turn at Gly-Asp) and the type SI (γ turn at Gly and βII′ turn at bicyclic template) geometries do not appear to take part in the conformational equilibrium of mimic **30**. Such findings are supported by the NMR analysis (see below) and are in agreement with the behavior previously observed for the corresponding unsubstituted cyclic RGD pentapeptide mimic.[23]

During the MC/SD calculation, compound **31**, which contains the poor β turn inducer bicyclic lactam 6,5-*trans* R, preferentially adopts extended geometries, as indicated by the Cβ-(Arg)–Cβ(Asp) average distance of 8.99 Å, featuring the SIV and the SIII conformations for 66% and 8% of the simulation, respectively. Thus, the mimic **31**, like the corresponding unsubstituted cyclic RGD pentapeptide mimic,[23] behaves in solution like an almost rigid system, preferring to adopt an extended RGD conformation represented by the type SIV geometry.

Compound **33** shows the maximum degree of backbone flexibility among the compounds studied, by adopting three different cyclopeptide geometries. According to the MC/SD results, the SIV type geometry is populated by 27%, the type SIII geometry by 24%, and the type SII geometry by 18%. In particular, with respect to the analogue ST1646 (see Figure 1), owing to the presence of the substituent on the lactam ring, mimic **33** seems to show more flexibility at conformational equilibrium. Finally, compound **32** adopts the extended type SIV geometry for 96% of the simulation, confirming the MC/EM view of a single possible backbone conformation for such type of functionalized scaffold.

The MC/EM and MC/SD calculations performed on the amide derivatives **42**–**44** and the ester derivative **45** (data not shown) revealed the same conformational preferences of the corresponding mimics **30**–**33**, suggesting that the nature of the substituent on the lactam ring should not affect the conformations of the cyclopentapeptide system.

Docking studies

To interpret, on a molecular basis, the affinity of compounds **30**–**33** and **42**–**45** for the $\alpha_v\beta_3$ receptor, docking studies were performed by starting from the low-energy cyclopeptide backbone conformations obtained from computational studies (free-state molecular mechanics conformational searches and molecular dynamics simulations). The Glide program (version 4.5) employed in docking calculations holds the protein rigid, while permitting torsional flexibility of the ligand.[27] However, during the docking process, the Glide program considers the cyclopeptide as a rigid body and prevents switching between backbone conforma-

Table 4. Population of the four SI–SIV type geometries during the 10-ns MC/SD simulations (AMBER*, H_2O GB/SA) of the cyclic RGD pentapeptide mimics **30**–**33** *cyclo*-(Arg-Gly-Asp-lactam).

Geometries	Percent of structures[a]			
	30	**31**	**32**	**33**
type SI γ(Gly)/βII′(lactam)	0	0	0	1
type SII γ(Gly)/βII′(Gly,Asp)[b]	57	2	0	18
type SIII inverse γ(Asp)/βII′(Gly,Asp)[b]	1	8	0	24
type SIV inverse γ(Asp)/βI(Pro,Arg)	29	66	96	27

[a]Percentage of conformations sampled during the simulation in which both the hydrogen bonds for γ turn (H–O distance: <3 Å) and for β turn (H–O distance: <4 Å) are formed. [b] Distorted type II′ β turn.

tions, whereas the side chains remain free to rotate (see Experimental Section for computational details).

The crystal structure of the extracellular segment of integrin $\alpha_v\beta_3$ in complex with the cyclic pentapeptide ligand EMD121974 (PDB code: 1L5G) was taken as a reference model for the interpretation of the docking results in terms of the ligand-bound conformation and ligand–protein interactions.[8] In the X-ray crystal structure, the potent $\alpha_v\beta_3$ antagonist EMD121974, bound to the head group of the integrin, features a specific conformation characterized by the formation of an inverse γ turn at Asp ($i+1$) position and a distorted βII′ turn at Gly, Asp, ($i+1$) and ($i+2$) positions, respectively. Indeed, the RGD sequence in this bound conformation is almost extended, with a Cβ(Arg)–Cβ(Asp) distance of 8.9 Å. The type SIII geometry obtained in our calculations for the cyclopentapeptide mimics **30**–**33** is very similar to the bioactive conformation experimentally observed for EMD121974 bound to $\alpha_v\beta_3$. The root-mean-square deviation (rmsd) of the RGD backbone atoms between the type SIII conformation of **33a** and the crystallographic structure of EMD121974 is 0.16 Å.

In the crystal complex, EMD121974 binds to the interface of the α and β units, forming specific electrostatic interactions. The acidic and basic pharmacophore groups and their orientation are essential for binding to $\alpha_v\beta_3$ because they act like an electrostatic clamp, attaching to charged regions of the binding site of the receptor. The positively charged Arg guanidinium group of EMD121974 interacts with the negatively charged side chains of Asp218 and Asp150 in the α unit. One carboxylate oxygen atom of the Asp side chain is coordinated to the metal cation in the metal-ion-dependent adhesion site (MIDAS) region of the β unit, while the second carboxylate oxygen atom forms hydrogen bonds with the backbone amides of Asn215 and Tyr122 in the β unit. The acidic and basic moieties of the RGD sequence point in opposite directions, effecting a separation of 14.2 Å between the barycenter of positive and negative charges, represented by the carbon atoms of the carboxylate group of Asp and of the guanidinium group of Arg, respectively. Further stabilizing interactions can occur that involve the formation of hydrogen bonds between the ligand backbone NH group of the Asp residue and the backbone carbonyl group of Arg216 in the β unit.

Assuming that the X-ray crystal structure pose describes the best interaction mode with the $\alpha_v\beta_3$ receptor, the top-ranked poses resulting from docking calculations for the conformers of compounds **30**–**33** are evaluated for their ability to reproduce the crystal structure model of binding. For mimic **30**, docking calculations starting from the type SI and SII geometries produced top-ranked poses, conserving only one of the two important electrostatic interactions with the $\alpha_v\beta_3$ receptor. The short Cβ(Arg)–Cβ(Asp) distances of the type SI and SII geometries probably prevent the guanidine and carboxyl groups from achieving the required separation for binding to the $\alpha_v\beta_3$ integrin. Moreover, the γ turn at Gly prevents formation of the hydrogen bond with Arg216 in the β unit. On the other hand, starting from the type SIV geometry featuring a more extended RGD sequence, top-ranked poses of compound **30** in $\alpha_v\beta_3$ reproduce all the important interactions of EMD121974 in the crystal structure, but show the CH_2OH group directed toward the integrin surface.

In light of such considerations, the micromolar affinity of mimic **30** for $\alpha_v\beta_3$ (Table 1) can be explained in terms of its low pre-organization for binding. In fact, as determined by computational and NMR studies (see below), compound **30** in solution mainly features the kinked-RGD type SII geometry which, according to the docking results previously discussed, is not able to properly fit into $\alpha_v\beta_3$ receptor due to the short Cβ-(Arg)–Cβ(Asp) distance and the inside amide orientation of the Asp NH group (γ turn at Gly).

Compound **31** is the most active mimic of the series ($IC_{50}=53.7\pm17.3$ nM for $\alpha_v\beta_3$). Automated docking calculations starting from SIII and SIV cyclopeptide conformations produce poses that conserve all the interactions observed in the X-ray crystal structure (Figure 5). The 6,5-*trans* scaffold drives the substituent in the direction of the aromatic ring of the Phe residue of EMD121974, that is, toward the outside of the integrin binding site, allowing the hydroxy group to fit unhindered.

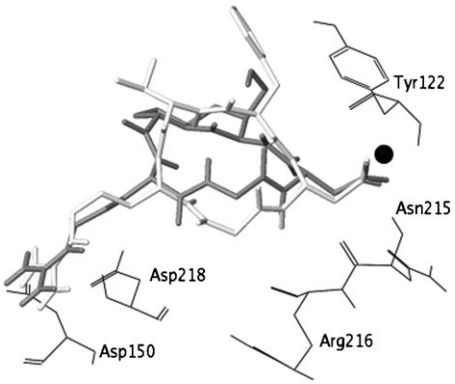

Figure 5. Top-ranked binding mode of ligand **31** (gray tube representation, type SIV inverse γ(Asp)/β(Pro-Arg) conformation of the cyclopeptide backbone) in the crystal structure of the extracellular domain of $\alpha_v\beta_3$ integrin overlayed on the bound conformation of EMD121974 (white tube representation). Selected integrin residues involved in the interactions with the ligand are shown in wire representation. The Mn^{2+} ion at MIDAS is shown as a black CPK sphere. Nonpolar hydrogen atoms are removed for clarity.

Thus, the type SIV geometry obtained from the molecular modeling calculations might represent an alternative ligand conformation suitable for binding to the $\alpha_v\beta_3$ receptor with respect to the experimental geometry of EMD121974 in the crystal complex. In fact, such type SIV geometry differs from the crystallographic binding conformation, that is, the type SIII geometry, only for the Gly amide proton orientation, maintaining all the key crystallographic interactions with the integrin binding site.

Because compound **31**, according to the computational and NMR studies (see below), mainly adopts the type SIV geometry in solution, the high affinity for $\alpha_v\beta_3$ can be attributed to its high structural pre-organization. However, compound **31** was shown to have lower affinity for $\alpha_v\beta_3$ than ST1646 (see Biological evaluation section above), which is probably due to the presence of a minor contribution from the SII type geometry

at conformational equilibrium (see NMR discussion reported below).

Compound **33**, with an IC_{50} value of 460 ± 126 nM, shows an intermediate affinity for $\alpha_v\beta_3$ relative to compounds **30** and **31**. This could be related to the major flexibility of this compound (see Tables 3 and 4), in particular to the participation of the type SII geometry in the conformational equilibrium of this mimic. The docking results starting from the SII, SIII, and SIV conformations of compound **33** reproduce the behavior observed for the corresponding conformers of mimic **30** and **31** (data not shown).

Finally, mimic **32**, with an IC_{50} value of 88 ± 7 nM, can be considered a good affinity ligand for $\alpha_v\beta_3$ due to its high pre-organization for binding. In fact, according to the modeling studies in solution, mimic **32** seems to adopt only the type SIV geometry that forms all key crystallographic interactions in the top-ranked poses of the docking calculation. The lower affinity toward $\alpha_v\beta_3$ with respect to the mimic **31** can be explained by considering the different orientation of the substituent on the lactam ring in the binding site. In fact, as already observed for mimic **30**, which incorporates the 6,5-*cis* scaffold, the 7,5-*cis* scaffold directs the hydroxy group toward the binding pocket, leading to potentially unfavorable contacts.

Regarding amide derivatives **42**–**44** and ester **45**, only docking calculations starting from the type SIII and SIV geometries are discussed. In fact, as already observed in the docking studies of mimics **30**–**33**, the cyclopeptide type SII γ(Gly)/β(Gly-Asp) conformation does not ensure the proper RGD disposition for binding to the receptor.

Compounds **42** and **45**, which respectively incorporate the functionalized 6,5-*cis* and 7,5-*cis* scaffolds, have some difficulties in reproducing the interactions of the reference ligand EMD121974, even if a bound-like cyclopentapeptide geometry such as the type SIV geometry is considered. Docking results highlight the formation of some steric clashes between the amide or ester butyl chains and the chain β integrin residues in the top-ranked poses. Such unfavorable interactions due to the orientation of the lactam substituent toward the binding site could perturb the binding of the RGD motif to $\alpha_v\beta_3$ and lead to loss of the interactions observed in the crystal structure. Docking results for compounds **42** and **45** agree with the experimentally determined high-micromolar binding affinity to $\alpha_v\beta_3$ (Table 1). In light of such findings, and in view of developing conjugates by starting from functionalized scaffolds, the 6,5-*cis*- and 7,5-*cis*-azabicycloalkanes do not appear as promising scaffolds for our purpose.

Compound **43**, which contains the functionalized 6,5-*trans* scaffold, is the most active ligand of the amide series, with an IC_{50} value of 114 ± 59 nM for $\alpha_v\beta_3$. Docking results for the type SIV geometry show that the ligand forms all the crystallographic interactions in the top-ranked poses and that the substituent of the lactam ring points toward the outside of the binding site without hindrance from the receptor (Figure 6). Docking results of compound **44** agree with the experimental micromolar binding affinity for $\alpha_v\beta_3$ (Table 1). The mimic in the type SIV geometry fails to form the interactions described in the crystal complex even in the top-ranked poses, probably due to some unfavorable amide chain contacts with receptor residues.

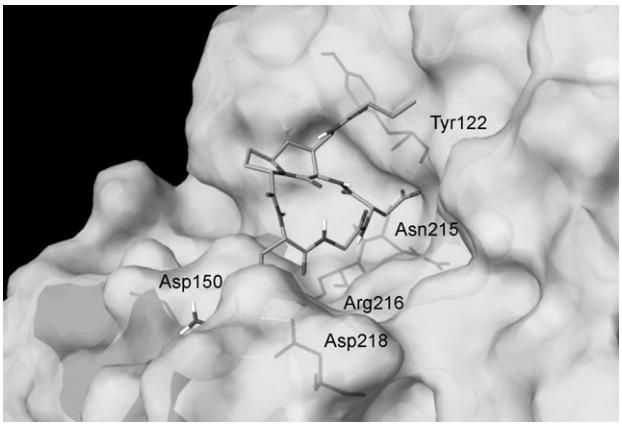

Figure 6. Top-ranked binding mode of ligand **43** (tube representation, type SIV inverse γ(Asp)/β(Pro-Arg) conformation of the cyclopeptide backbone) in the crystal structure of the extracellular domain of $\alpha_v\beta_3$ integrin represented as a molecular surface. Selected integrin residues involved in the interactions with the ligand are shown in gray tube representation. Nonpolar hydrogen atoms are removed for clarity.

Therefore, in view of these findings, the RGD ligand **31**, containing the functionalized 6,5-*trans* scaffold, is a suitable candidate for the conjugation of molecular entities for therapeutic and diagnostic applications. Its amide derivative **43** maintains a nanomolar binding affinity to $\alpha_v\beta_3$ thanks to both the conformational pre-organization of the RGD sequence and the ability to properly orient the side chain conjugated to the scaffold.

NMR studies

Compounds **30** and **31** were characterized by NMR spectroscopy in H_2O/D_2O solution at 298 K. A conformational study was performed using standard 2D NMR NOESY experiments and studying the chemical shifts and the temperature variation of amide protons (see Supporting Information).

For compound **30**, these studies suggest that the lactam NH group (Lact-NH; $\delta = 7.81$ ppm) is involved in an intramolecular hydrogen bond, while Gly-NH ($\delta = 8.85$ ppm) is solvent exposed. The behavior of Arg-NH ($\delta = 7.18$ ppm) is typical of a non-hydrogen-bound and non-solvated proton. The NOESY data show the following significant long-range cross-peaks (Figure 7): Lact-NH/Asp-NH (medium), Gly-Hα_1/Asp-NH (weak), and Lact-Hβ/Pro-Hδ (medium). Therefore, the amide protons Asp-NH and Lact-NH must be inside the pentapeptide ring and experience a hydrogen bond contact. Lact-NH binds to the carbonyl group of Arg, stabilizing a slightly distorted β turn, and Asp-NH binds to the same carbonyl group to stabilize a γ turn at Gly. In this preferred conformation, the lactam ring appears to adopt a pseudo-chair conformation in which the CH_2OH moiety is in a pseudo-equatorial conformation. The presence of the CH_2OH moiety on the bicyclic lactam does not affect the conformational behavior of the pseudo-cyclopentapeptide **30**, which is very similar to that of the analogue compound without this functionalization.[28]

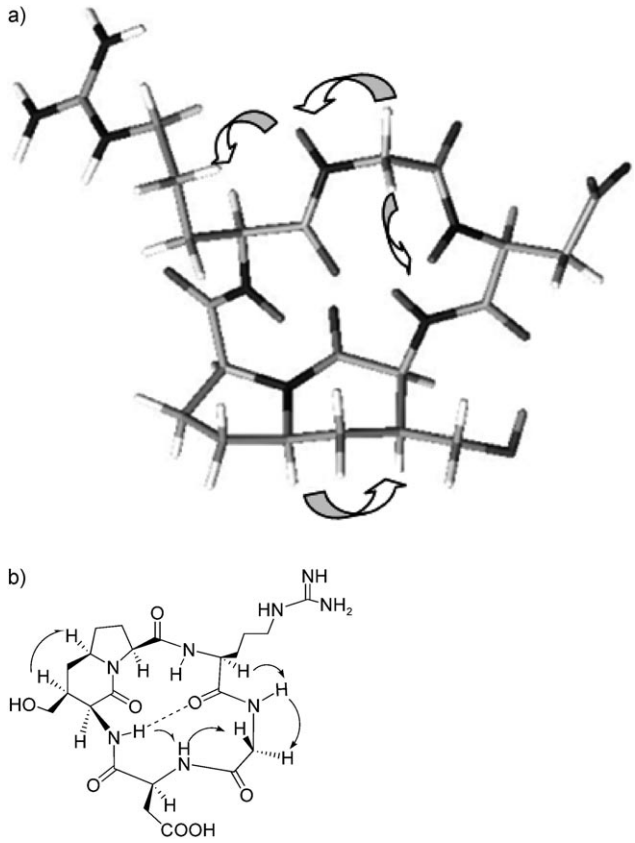

Figure 7. a) Preferred conformation of **30** sampled during the 10-ns MC/SD simulation after energy minimization, in agreement with spectroscopic data (type SII γ(Gly)/distorted βII′(Gly-Asp) geometry). b) Significant long-range NOE contacts of compound **30** in H_2O/D_2O solution.

The preferred solution conformation of the cyclopentapeptide ring of mimic **30** is in agreement with the most populated geometry sampled during the 10-ns MC/SD simulations (type SII geometry, 57% of the structures, Table 4). A Cβ(Arg)–Cβ-(Asp) mean distance of 8.0 Å is calculated from the structures sampled during the simulations and features the type SII γ-(Gly)/distorted βII′(Gly-Asp) geometry.

Both experimental and computational results indicate that mimic **30** prefers to adopt the SII type geometry with a strong kink in the RGD motif, although participation of the type SIV cyclopeptide arrangement in the conformational equilibrium is observed during the MC/SD simulation (Table 4). However, the binding affinity of compound **30** for $\alpha_V\beta_3$ integrin and docking studies in the same receptor suggest that the contribution of type SIV should be smaller than the calculations show.

For compound **31**, analysis of the amide proton chemical shifts and the temperature variation of amide protons suggests that Gly-NH ($\delta = 7.7$ ppm) and Lact-NH ($\delta = 7.58$ ppm) are involved in an intramolecular hydrogen bond, while Asp-NH ($\delta = 9.19$ ppm) and Arg-NH ($\delta = 8.42$ ppm) are solvent exposed. A more detailed conformational study was undertaken with NOESY data. We observed an intense cross-peak due to the correlation between Pro-Hδ and Lact-Hα; this contact is achievable only if the lactam is forced into a pseudo-boat conformation (Figure 8) so that Pro-Hδ and Lact-Hα occupy a pseudo-axial position in the ring structure. The observed Pro-Hδ/Lact-Hγ coupling constant (13 Hz) concurs with this. As a result, the bicyclic scaffold sets the RGD backbone in a pseudo-equatorial conformation, modulating the distance between the side chains of Arg and Asp, a key factor in the specificity of ligand binding (Figure 8).

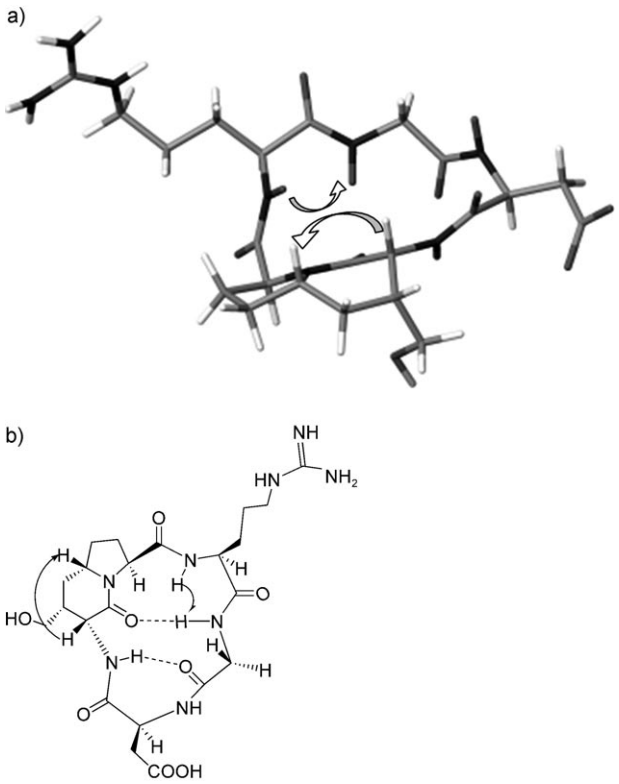

Figure 8. a) Preferred conformation of **31** sampled during the 10-ns MC/SD simulation after energy minimization, in agreement with spectroscopic data (type SIV inverse γ(Asp)/βI(Pro-Arg) geometry). b) Significant long-range NOE contacts of compound **31** in H_2O/D_2O solution.

Moreover, the NOESY data for **31** show NOEs between Gly-NH and Arg-NH (strong) and between Asp-NH and Lact-NH (weak). These are exclusive NOEs and support the presence of two different conformations, with one preferred over the other. The Gly-NH/Arg-NH NOE contact and the chemical shift values of Gly-NH are indicative of a β turn conformation stabilized by a hydrogen bond between Gly-NH and the lactam C=O (Figure 8b. This preferred conformation is also stabilized by a hydrogen bond between Lact-NH and the carbonyl group of Gly, giving rise to a γ turn centered on the aspartic acid residue, in accordance with the computational results. The chemical shift value (7.78 ppm) of the amide proton Lact-NH and the NOE contact between Asp-NH and only one Gly-Hα support this conformational motif. The presence of β(Pro-Arg) and γ-(Asp) turns stabilize a cyclopeptide geometry characterized by an RGD extended conformation (Figure 8a. All these data provide experimental evidence toward the participation of the calculated type SIV cyclopeptide arrangement in the conformational equilibrium of compound **31**. Moreover, the NOEs be-

tween Asp-NH and Lact-NH (weak) are indicative of a different conformation in which the Lact-NH and Asp-NH amide protons point inside the pentapeptide, and Asp-NH experiences a hydrogen bond with Arg C=O, stabilizing a γ turn centered on the glycine residue (type SII geometry). Although the participation of this geometry in the conformational equilibrium of ligand **31** is underestimated by computational modeling, the NMR results offer an explanation for the IC_{50} value of 53.7 nM toward the $\alpha_v\beta_3$ receptor.

The preferred solution conformation of the cyclopentapeptide ring of mimic **31** is in agreement with the most populated geometry sampled during the 10-ns MC/SD simulations (type SIV geometry, 66% of the structures, Table 4). A Cβ(Arg)–Cβ-(Asp) mean distance of 9.2 Å is calculated from the structures sampled during the simulations, and features the type SIV inverse γ(Asp)/βI(Pro-Arg) geometry.

Conclusions

A series of eight cyclic RGD-containing functionalized azabicycloalkane peptides were synthesized, and their binding toward $\alpha_v\beta_3$ and $\alpha_v\beta_5$ receptors was evaluated. Conformational analysis of the aforementioned series, performed by computational and NMR studies, showed similar results to the corresponding cyclopentapeptides containing an unsubstituted scaffold.

Among the new series, compound **31** showed the highest affinity for $\alpha_v\beta_3$ and $\alpha_v\beta_5$ integrins. The conformational analysis of cyclic RGD peptide **31** showed a preferred backbone geometry similar to the conformation of EMD121974 bound to the $\alpha_v\beta_3$ receptor and characterized by an almost extended RGD disposition.

Compound **31** was determined to be highly pre-organized for binding to $\alpha_v\beta_3$ integrin, and docking studies confirmed its ability to form all the key interactions within the binding site. However, mimic **31** showed slightly less activity toward $\alpha_v\beta_3$ than reference compound ST1646, a potent antagonist previously synthesized by our research group. The activity of compound **31** toward $\alpha_v\beta_3$ is probably influenced, at solution equilibrium, by the presence of a less significant conformation unsuitable for binding to $\alpha_v\beta_3$, as detected by NMR studies. Nevertheless, the possibility of conjugation while maintaining the binding activity offered by the new scaffold (the corresponding amide derivative **43** maintains activity at the nanomolar level) suggests that this functionalized RGD cyclic peptide could be a suitable system for targeted drug delivery and for diagnostic applications. Docking studies of derivative **43** confirm that the 6,5-*trans* scaffold properly orients the substituent on the lactam ring within the binding site of $\alpha_v\beta_3$, maintaining the interactions observed in the reference crystallographic complex.

Moreover, experiments on cellular models indicate that compound **31** acts efficiently as an $\alpha_v\beta_3/\alpha_v\beta_5$ integrin antagonist by interfering with both cell adhesion and migration on vitronectin in the absence of any evident cytotoxic activity.

Experimental Section

Chemical procedures

General: All chemicals and solvents were of reagent grade and were used without further purification. Solvents were dried by standard procedures, and reactions requiring anhydrous conditions were performed under N_2 or Ar atmospheres. Optical rotations $[\alpha]_D$ were measured using a PerkinElmer 241 polarimeter with a cell of 1 dm path length and 1 mL capacity. ^1H and ^{13}C NMR spectra were recorded at 300 K on a Bruker Avance 400 or 600 MHz spectrometer. Chemical shifts (δ) are expressed in parts per million (ppm) relative to internal Me_4Si as standard. Mass spectra were obtained with an ESI apparatus (Bruker Esquire 3000 plus). Thin-layer chromatography (TLC) was carried out with pre-coated Merck F_{254} silica gel plates. Flash chromatography (FC) was carried out with Macherey–Nagel silica gel 60 (230–400 mesh). Reversed-phase column chromatography was carried out with the Biotage SP1 or SP4 systems using Biotage 25+M C_{18} cartridges. Semipreparative HPLC was carried out on a Waters SymmetryPrep C_{18} 7 μm 7.8×300 mm column, or a Waters Atlantis C_{18} OBD 5 μm 19 mm×10 cm column, or a Supleco Ascentis RPAmide 5 μm 21.1 mm×15 cm column; the gradient used was from 0.1% TFA in H_2O to 0.1% TFA in H_2O/MeCN (75:25 *v/v*) over 30 min. Elemental analyses were performed by the staff of the microanalytical laboratory of our department, and the results are within ±0.4% of the calculated values unless otherwise stated.

General procedure A: synthesis of Temp-Arg(Pmc)-Gly-OMe. TFA (9.3 mL, 125 mmol) was added to a solution of bicyclic lactam template **6**–**9** (2.50 mmol) in CH_2Cl_2 (25 mL). The reaction mixture was stirred at room temperature for ~2 h. After reaction completion, the solvent was evaporated under reduced pressure. The crude product underwent the following reaction without further purification: DIC (424 μL, 2.74 mmol) and HOBt (405 mg, 3 mmol) were added to a solution of the crude (2.50 mmol) in dry THF (20 mL) under Ar at room temperature. The mixture was stirred for ~20 min. A solution of dipeptide HO-Arg(Pmc)-Gly-OMe (1.9 g, 3.73 mmol) in dry CH_2Cl_2 (5 mL) was then added. The reaction mixture was stirred at room temperature for ~18 h, and was then filtered trough a pad of Celite and washed with THF. The collected organic phase was evaporated under reduced pressure. The crude was dissolved in EtOAc and washed with 5% $NaHCO_3$. The organic layer, dried with Na_2SO_4, was evaporated under reduced pressure, and the crude was purified by FC.

Compound 14. The pure product was obtained after FC ($CHCl_3$/MeOH 98:2). Yield: 30%; white foam; $[\alpha]_D^{22} = -44.7$ ($c = 1.00$, $CHCl_3$); ^1H NMR (400 MHz, $CDCl_3$): $\delta = 1.32$ (s, 6H, C(*CH*$_3$)$_2$ Pmc), 1.53–1.70 (m, 2H, 2*H*γ Arg), 1.70–1.87 (m, 4H, *H*-5, *H*β Arg, *CH*$_2$CH$_2$Ar Pmc), 1.97 (m, 1H, *H*-7), 2.0–2.18 (m, 6H, *H*β Arg, *H*-8, *H*-7, C*H*$_3$ Pmc), 2.18–2.28 (m, 2H, *H*-5, *H*-8), 2.56 (s, 3H, C*H*$_3$ Pmc), 2.58 (s, 3H, C*H*$_3$ Pmc), 2.64 (t, 2H, $J = 6.8$ Hz, CH$_2$*CH*$_2$Ar Pmc), 3.02–3.18 (m, 2H, *H*-4, *H*δ Arg), 3.38 (m, 1H, *H*δ Arg), 3.50 (m, 1H, *H*-3), 3.68 (m, 1H, *H*-6), 3.68 (s, 3H, C*H*$_3$*O*), 3.73 (m, 1H, *H*CHO), 4.02 (m, 2H, C*H*$_2$Ph), 4.12 (m, 1H, *H*α Gly), 4.32 (t, 1H, $J = 8.0$ Hz, *H*CHO), 4.44 (d, 1H, $J = 8.0$ Hz, *H*-9), 4.49–4.60 (m, 2H, *H*α Arg, *H*α Gly), 6.12 (bs, 1H, (N*H*)$_2$C=N*H*), 6.36 (bs, 2H, (N*H*)$_2$C=N*H*), 7.25–7.32, (m, 3H, aromatic protons), 7.32–7.50 (m, 4H, 2 aromatic protons, N*H* Arg, N*H* Gly); ^{13}C NMR (100.6 MHz, $CDCl_3$): 172.5, 171.6, 170.2, 167.9, 156.5, 153.6, 136.5, 135.6, 134.9, 134.0, 129.7, 128.4, 127.7, 124.0, 118.0, 73.7, 71.6, 64.8, 62.3, 60.2, 59.3, 53.0, 52.3, 42.6, 41.3, 40.5, 33.0, 32.8, 31.4, 29.9, 29.1, 27.0, 24.8, 21.6, 18.7, 17.7, 12.3; MS (ESI^+) *m/z*: 810.7 $[M+H]^+$; Anal.: ($C_{40}H_{55}N_7O_9S$) C, H, N.

Compound 15. The pure product was obtained after FC ($CHCl_3$/*i*PrOH 9:1). Yield: 90%; white foam; $[\alpha]_D^{22} = -6.24$ ($c = 1.00$, $CHCl_3$); ^{1}H NMR (400 MHz, [D$_6$]acetone): $\delta = 1.30$ (s, 6H, C(CH_3)$_2$ Pmc), 1.35 (m, 1H, *H*-5), 1.58 (m, 1H, *H*-7), 1.6–1.76 (m, 3H, 2*H*γ Arg, *H*β Arg), 1.83 (t, 2H, $J = 6.8$ Hz, CH_2CH_2Ar Pmc), 1.91 (m, 1H, *H*-8), 1.99 (m, 1H, *H*β Arg), 2.1 (s, 3H, CH_3 Pmc), 2.14 (m, 1H, *H*-5), 2.17 (m, 1H, *H*-7), 2.34 (m, 1H, *H*-8), 2.57 (s, 3H, CH_3 Pmc), 2.59 (s, 3H, CH_3 Pmc), 2.66 (t, 2H, $J = 6.8$ Hz, CH_2CH_2Ar Pmc), 3.0 (m, 1H, *H*-4), 3.20–3.29 (m, 2H, *H*δ Arg), 3.32 (m, 1H, *H*-3), 3.45 (dd, 1H, $J = 8.0$ Hz, $J = 8.4$ Hz, *H*CHO), 3.67 (s, 3H, CH_3O), 3.82 (d, 1H, $J = 14.4$ Hz, *H*CHPh), 3.86 (m, 1H, *H*-6), 3.96 (m, 2H, 2*H*α Gly), 4.09 (dd, 1H, $J = 8.0$ Hz, $J = 7.6$ Hz, *H*CHO), 4.5–4.65 (m, 3H, *H*-9, *H*α Arg, *H*CHPh), 6.41 (bs, 1H, (N*H*)$_2$C=N*H*), 6.60 (bs, 2H, (N*H*)$_2$C=N*H*), 7.21, (m, 1H, aromatic proton), 7.27 (m, 2H, aromatic protons), 7.36 (m, 2H, aromatic protons), 7.76 (d, 1H, $J = 8.0$ Hz, N*H* Arg), 7.83 (m, 1H, N*H* Gly); ^{13}C NMR (100.6 MHz, [D$_6$]acetone): $\delta = 172.5$, 172.1, 170.9, 168.3, 157.3, 153.7, 139.5, 136.0, 135.4, 129.8, 128.6, 127.5, 124.0, 118.7, 74.3, 71.4, 66.1, 63.0, 61.3, 60.2, 53.1, 52.1, 42.8, 41.4, 41.1, 33.8, 33.4, 33.2, 29.7, 29.1, 26.9, 26.1, 21.9, 18.8, 17.7, 12.3; MS (ESI$^+$) *m/z*: 848.3 [*M*+K]$^+$, 832.5 [*M*+Na]$^+$, 810.8 [*M*+H]$^+$; Anal.: ($C_{40}H_{55}N_7O_9S$) C, H, N.

Compound 16. The pure product was obtained after FC (EtOAc/*i*PrOH 95:5→9:1). Yield: 77%; white foam; $[\alpha]_D^{22} = -48.9$ ($c = 1.00$, $CHCl_3$); ^{1}H NMR (400 MHz, [D$_6$]acetone): $\delta = 1.32$ (s, 6H, C(CH_3)$_2$ Pmc), 1.52–1.78 (m, 4H, 2*H*γ Arg, *H*β Arg, *H*-5) 1.78–1.94 (m, 4H, 2*H*-6, CH_2CH_2Ar Pmc), 1.95–2.18 (m, 6H, *H*β Arg, 2*H*-9, *H*-5, CH_3 Pmc), 2.25 (m, 1H, *H*-8), 2.55 (s, 3H, CH_3 Pmc), 2.56 (m, 1H, *H*-4), 2.57 (s, 3H, CH_3 Pmc), 2.67 (m, 2H, CH_2CH_2Ar Pmc), 3.21 (m, 1H, *H*δ Arg), 3.27 (m, 1H, *H*δ Arg), 3.50–3.62 (m, 2H, *H*CHO, *H*-3), 3.68 (s, 3H, CH_3O), 3.76 (m, 1H, *H*CHPh), 3.90–4.06 (m, 3H, 2*H*α Gly, *H*CHO), 4.09 (m, 1H, *H*-7), 4.26 (m, 1H, *H*CHPh), 4.62 (m, 1H, *H*α Arg), 4.69 (m, 2H, *H-10*), 6.34 (bs, 1H, (N*H*)$_2$C=N*H*), 6.68 (bs, 2H, (N*H*)$_2$C=N*H*), 7.20–7.32 (m, 3H, aromatic protons), 7.32–7.42 (m, 2H, aromatic protons), 7.51 (m, 1H, N*H* Arg), 7.78 (m, 1H, N*H* Gly); ^{13}C NMR (100.6 MHz, [D$_6$]acetone): $\delta = 171.4$, 171.1, 170.0, 169.8, 156.5, 152.7, 137.5 135.4, 135.1, 134.5, 129.2, 127.9, 127.0, 72.8, 71.2, 61.8, 61.6, 59.1, 51.8, 51.3, 45.3, 40.6, 39.8, 37.8, 33.2, 33.0, 32.6, 31.0, 29.2, 27.0, 26.1, 24.9, 21.1, 18.0, 16.8, 11.4; MS (ESI$^+$) *m/z*: 824.4 [*M*+H]$^+$; Anal.: ($C_{41}H_{57}N_7O_9S$) C, H, N.

Compound 17. The pure product was obtained after FC ($CHCl_3$/MeOH 95:5). Yield: 90%; white foam; $[\alpha]_D^{22} = +15.1$ ($c = 1.00$, $CHCl_3$); ^{1}H NMR (400 MHz, [D$_6$]acetone): $\delta = 1.3$ (s, 6H, C(CH_3)$_2$ Pmc), 1.53–1.68 (m, 3H, *H*-6, 2*H*γ Arg) 1.69–1.78 (m, 3H, *H*β Arg, *H*-5, *H*-8), 1.80 (m, 1H, *H-6*), 1.82 (m, 2H, CH_2CH_2Ar Pmc), 1.9–2.0 (m, 2H, *H*β Arg, *H*-9), 2.05 (m, 1H, *H*-5), 2.08 (s, 3H, CH_3 Pmc), 2.2 (m, 1H, *H*-9), 2.35 (m, 1H, *H*-8), 2.51 (m, 1H, *H*-4), 2.56 (s, 3H, CH_3 Pmc), 2.58 (s, 3H, CH_3 Pmc), 2.64 (m, 2H, CH_2CH_2Ar Pmc), 3.13 (m, 1H, *H*δ Arg), 3.24 (m, 1H, *H*δ Arg), 3.48 (t, 1H, $J = 7.5$ Hz, *H*CHO), 3.53 (m, 1H, *H*-3), 3.54 (s, 3H, CH_3O), 3.69 (m, 1H, *H*CHPh), 3.85–3.92 (m, 2H, 2*H*α Gly), 3.94 (t, 1H, $J = 8.0$ Hz, *H*CHO), 4.14–4.23 (m, 2H, *H*CHPh, *H-7*), 4.57 (m, 1H, *H*α Arg), 4.6 (m, 2H, *H-10*), 6.6 (bs, 1H, (N*H*)$_2$C=N*H*), 6.68 (bs, 2H, (N*H*)$_2$C=N*H*), 7.15–7.27 (m, 3H, aromatic protons), 7.33 (m, 2H, aromatic protons), 7.72 (d, 1H, $J = 8.2$ Hz, N*H* Arg), 7.86 (m, 1H, N*H* Gly); ^{13}C NMR (100.6 MHz, [D$_6$]acetone): $\delta =$ 171.9, 171.5, 170.3, 169.9, 156.5, 152.9, 135.2, 135.1, 134.6, 129.2, 127.8, 126.8, 73.4, 72.7, 71.0, 61.8, 61.2, 59.1, 52.4, 51.2, 45.54, 40.6, 40.5, 33.6, 32.7, 32.5, 31.0, 27.9, 27.2, 26.2, 26.1, 24.9, 21.1, 18.0, 16.9, 11.5; MS (ESI$^+$) *m/z*: 824.6 [*M*+H]$^+$; Anal.: ($C_{41}H_{57}N_7O_9S$) C, H, N.

General procedure B: synthesis of Z-Asp(*t*Bu)-Temp-Arg(Pmc)-Gly-OMe. Pd/C 10% (20% *w/w*) was added to a solution of compound **14**–**17** (0.22 mmol) in MeOH (5 mL). The reaction was stirred under H_2 (5 atm) for 3 days. After reaction completion, the mixture was filtered through a pad of Celite and washed with MeOH. The collected organic phase was evaporated under reduced pressure to yield the desired product as a white solid, which was used without further purification. DIC (37 μL, 0.241 mmol) and HOBt (32 mg, 0.24 mmol) were added to a solution of Z-Asp(*t*Bu)-OH (71 mg, 0.22 mmol) in dry THF (2 mL) under N_2 at room temperature. After 15 min, the mixture was cooled to −30 °C, and a solution of the crude compound (0.22 mmol) in dry THF (3 mL) was added dropwise. The reaction mixture was stirred at room temperature overnight. After completion, the mixture was filtered through a pad of Celite and washed with THF. The collected organic phase was evaporated under reduced pressure. The residue was dissolved in EtOAc and washed with 5% $NaHCO_3$. The solvent, dried with Na_2SO_4, was evaporated, and the crude was purified by FC to yield the desired product.

Compound 18. The pure product was obtained after FC (CH_2Cl_2/acetone 1:1). Yield: 87%; white foam; $[\alpha]_D^{22} = -22.2$ ($c = 1.00$, $CHCl_3$); ^{1}H NMR (400 MHz, [D$_6$]acetone): $\delta = 1.31$ (s, 6H, C(CH_3)$_2$ Pmc), 1.43 (s, 9H, C(CH_3)$_3$), 1.50–1.73 (m, 5H, 2*H*γ Arg, *H*β Arg *H*-7, *H*-5), 1.86 (t, 2H, $J = 6.8$ Hz, CH_2CH_2Ar Pmc), 2.02 (m, 1H, *H*β Arg), 2.10 (s, 3H, CH_3 Pmc), 2.16 (m, 1H, *H*-8), 2.23–2.36 (m, 2H, *H*-8, *H*-7), 2.53 (m, 1H, *H*-5), 2.57 (s, 3H, CH_3 Pmc), 2.59 (s, 3H, CH_3 Pmc), 2.67 (t, 2H, $J = 7.0$ Hz, CH_2CH_2Ar Pmc), 2.79 (m, 2H, 2*H*β Asp), 2.86 (m, 1H, *H*-4), 3.23 (m, 2H, 2*H*δ Arg), 3.40 (d, 1H, $J = 10.8$ Hz, HC*H*O), 3.65 (m, 1H, $J = 17.6$ Hz, $J = 3.6$ Hz, *H*α Gly), 3.76 (s, 3H, CH_3O), 3.88–4.00 (m, 2H, *H*-6, HC*H*O), 4.14 (m, 1H, $J = 17.6$ Hz, $J = 7.2$ Hz, *H*α Gly), 4.37–4.53 (m, 3H, *H*-3, *H*-9, *H*α Arg), 4.56 (m, 1H, *H*α Asp), 5.15 (s, 2H, CH_2Ph), 6.30 (bs, 1H, (N*H*)$_2$C=N*H*), 6.50 (bs, 2H, (N*H*)$_2$C=N*H*), 6.63 (m, 1H, N*H* Asp), 7.30–7.45 (m, 5H, aromatic protons), 7.58–7.67 (m, 2H, N*H* Temp, N*H* Gly), 7.85 (bs, 1H, N*H* Arg); ^{13}C NMR (100.6 MHz, [D$_6$]acetone): $\delta = 172.8$, 171.5, 171.0, 170.4, 170.3, 170.2, 156.3, 152.8, 137.0, 135.1, 134.6, 128.4, 127.9, 123.1, 117.8, 80.7, 73.4, 66.3, 61.4, 61.2, 60.6, 54.5, 52.1, 51.9, 51.7, 50.7, 50.6, 40.5, 40.3, 37.3, 36.3, 32.5, 31.7, 27.3, 26.1, 26.0, 21.1, 17.9, 16.8, 11.4; MS (ESI$^+$) *m/z*: 1027.7 [*M*+H]$^+$; Anal.: ($C_{49}H_{70}N_8O_{14}S$) C, H, N.

Compound 19. The pure product was obtained after FC (CH_2Cl_2/*i*PrOH 9:1). Yield: 84%; white foam; $[\alpha]_D^{22} = -33.0$ ($c = 1.00$, $CHCl_3$); ^{1}H NMR (400 MHz, [D$_6$]acetone): $\delta = 1.30$ (s, 6H, C(CH_3)$_2$ Pmc), 1.42 (s, 9H, C(CH_3)$_3$), 1.46 (m, 1H, *H*-5), 1.50 (m, 1H, *H*-7), 1.53–1.69 (m, 3H, 2*H*γ Arg, *H*β Arg), 1.83 (m, 2H, CH_2CH_2Ar Pmc), 1.9–2.02 (m, 2H, *H*-8, *H*β Arg), 2.03–2.08 (m, 1H, *H*-5), 2.1 (s, 3H, CH_3 Pmc), 2.17–20 (m, 1H, *H*-7, *H*-8), 2.44 (m, 1H, *H*-4), 2.56 (s, 3H, CH_3 Pmc), 2.58 (s, 3H, CH_3 Pmc), 2.62 (m, 1H, *H*β Asp), 2.68 (m, 2H, CH_2CH_2Ar Pmc), 2.85 (m, 1H, *H*β Asp), 3.2 (m, 2H, 2*H*δ Arg), 3.47 (m, 2H, CH_2O), 3.67 (s, 3H, CH_3O), 3.79–3.90 (m, 2H, *H*-6, O*H*), 3.94 (m, 2H, 2*H*α Gly), 4.47–4.57 (m, 2H, *H*α Arg, *H*-9), 4.58–4.65 (m, 2H, *H*-3, *H*α Asp), 5.10 (m 2H, CH_2Ph), 6.27 (bs, 1H, (N*H*)$_2$C=N*H*), 6.57 (bs, 2H, (N*H*)$_2$C=N*H*), 6.80 (m, 1H, N*H* Temp), 7.27–7.44 (m, 5H, aromatic protons), 7.65 (m, 1H, N*H* Arg), 7.74 (bs, 1H, N*H* Gly), 7.9 (bs, 1H, N*H* Asp); ^{13}C NMR (100.6 MHz, [D$_6$]acetone): $\delta = 172.6$, 172.5, 172.1, 170.9, 170.6, 169.2, 157.4, 157.0, 153.7, 138.0, 136.1, 135.9, 135.5, 129.2, 128.7, 124.0, 118.7, 81.4, 74.3, 67.1, 62.8, 61.2, 59.0, 53.0, 52.8, 52.2, 51.2, 41.5, 40.9, 39.7, 38.5, 33.4, 33.0, 30.0, 29.6, 28.3, 28.2, 27.0, 26.1, 22.0, 18.9, 17.8, 12.3; MS (ESI$^+$) *m/z*: 1049.0 [*M*+Na]$^+$, 1027.2 [*M*+H]$^+$; Anal.: ($C_{49}H_{70}N_8O_{14}S$) C, H, N.

Compound 20. The pure product was obtained after FC (EtOAc/*i*PrOH 9:1). Yield: 60%; white foam; $[\alpha]_D^{22} = -42.2$ ($c = 1.00$, $CHCl_3$); ^{1}H NMR (400 MHz, [D$_6$]acetone): $\delta = 1.32$ (s, 6H, C(CH_3)$_2$ Pmc), 1.42 (s, 9H, C(CH_3)$_3$), 1.57 (m, 1H, *H*-4), 1.60–1.76 (m, 4H, 2*H*γ Arg, *H*β Arg, *H*-6), 1.82 (m, 1H, *H-8*), 1.84 (m, 2H, CH_2CH_2Ar Pmc), 1.88–1.97

(m, 3H, *H*-6, *H*-5, β Arg), 1.97–2.05 (m, 2H, *H*-9, *H*-5), 2.10 (s, 3H, CH_3 Pmc), 2.12 (m, 1H, *H*-9), 2.27 (m, 1H, *H*-8), 2.57 (s, 3H, CH_3 Pmc), 2.59 (s, 3H, CH_3 Pmc), 2.66 (m, 2H, CH_2CH_2Ar Pmc), 2.75 (m, 1H, *H*β Asp), 2.85 (m, 1H, *H*β Arg), 3.22 (m, 2H, 2*H*δ Arg), 3.38 (m, 1H, *H*CHO), 3.59 (m, 1H, *H*CHO), 3.68 (s, 3H, CH_3O), 3.95 (m, 1H, *H*α Gly), 3.99–4.06 (m, 2H, *H*α Gly, *H*-7), 4.51 (m, 1H, *H*-3), 4.57 (m, 1H, *H*α Arg), 4.62 (m, 1H, *H*α Asp), 4.65 (m, 1H, *H-10*), 5.13 (m, 2H, CH_2Ph), 6.18 (bs, 1H, (N*H*)$_2$C=N*H*), 6.56 (bs, 2H, (N*H*)$_2$C=N*H*), 7.02 (bs, 1H, N*H* Asp), 7.30 (m, 1H, aromatic proton), 7.32–7.42 (m, 4H, aromatic protons), 7.68 (m, 1H, N*H* Temp), 7.78 (m, 1H, N*H* Gly), 8.04 (m, 1H, NH Arg); ^{13}C NMR (100.6 MHz, [D$_6$]acetone): δ = 171.8, 171.6, 171.3, 170.9, 170.0, 169.8, 156.5, 156.2, 152.9, 137.1, 135.2, 134.9, 134.6, 128.4, 127.8, 123.1, 117.8, 80.4, 73.4, 66.3, 63.7, 61.8, 58.7, 54.1, 52.3, 52.2, 51.3, 41.7, 40.6, 37.4, 32.9, 32.5, 31.1, 29.6, 27.3, 27.1, 26.1, 26.0, 21.1, 18.0, 16.9, 11.4; MS (ESI$^+$) *m/z*: 1041.5 [*M*+H]$^+$; Anal.: ($C_{50}H_{72}N_8O_{14}S$) C, H, N.

Compound 21. The pure product was obtained after FC (EtOAc/MeOH 9:1). Yield: 83%; white foam; $[\alpha]_D^{22} = -18.5$ (c = 1.00, $CHCl_3$); ^{1}H NMR (400 MHz, [D$_6$]acetone): δ = 1.31 (s, 6H, C(CH_3)$_2$ Pmc), 1.43 (s, 9H, C(CH_3)$_3$), 1.52–1.70 (m, 5H, 2*H*γ Arg, *H*β Arg, *H*-4, *H*-6), 1.76 (m, 1H, *H-8*), 1.80–1.88 (m, 3H, *H*-6, CH_2CH$_2$Ar Pmc), 1.89–1.98 (m, 3H, 2*H*-5, *H*β Arg), 2.06 (m, 1H, *H*-9), 2.10 (s, 3H, CH_3 Pmc), 2.2–2.35 (m, 2H, *H*-9, *H*-8), 2.57 (s, 3H, CH_3 Pmc), 2.59 (s, 3H, CH_3 Pmc), 2.62–2.70 (m, 3H, CH_2CH_2Ar Pmc, *H*β Asp), 2.86 (m, 1H, *H*β Arg), 3.20 (m, 2H, 2*H*δ Arg), 3.45 (m, 1H, *H*CHO), 3.61 (m, 1H, *H*CHO), 3.66 (s, 3H, CH_3O), 3.93 (m, 2H, 2*H*α Gly), 4.26 (m, 1H, *H*-7), 4.41 (m, 1H, *H*-3), 4.54–4.63 (m, 2H, *H*α Arg, *H-10*), 4.69 (m, 1H, *H*α Asp), 5.12 (m, 2H, CH_2Ph), 6.3 (bs, 1H, (N*H*)$_2$C=N*H*), 6.5 (bs, 2H, (N*H*)$_2$C=N*H*), 6.81 (m, 1H, N*H* Asp), 7.28–7.42 (m, 5H, aromatic protons), 7.52 (m, 1H, N*H* Temp), 7.58 (m, 1H, N*H* Gly), 8.05 (m, 1H, NH Arg); ^{13}C NMR (100.6 MHz, [D$_6$]acetone): δ = 171.8, 171.7, 171.5, 170.9, 170.4, 169.6, 156.3, 156.1, 152.8, 137.0, 135.2, 135.0, 134.6, 128.4, 127.8, 123.1, 117.8, 80.5, 73.4, 66.2, 63.7, 61.4, 58.7, 54.8, 52.5, 51.8, 51.4, 41.3, 40.6, 37.5, 32.8, 32.5, 32.1, 30.4, 29.5, 29.3, 27.3, 26.7, 26.1, 25.7, 21.1, 17.9, 16.8, 11.4; MS (ESI$^+$) *m/z*: 1041.7 [*M*+H]$^+$; Anal.: ($C_{50}H_{72}N_8O_{14}S$) C, H, N.

General procedure C: synthesis of Z-Asp(*t*Bu)-Temp-Arg(Pmc)-Gly-OBn. Benzyl alcohol (12 mL, 113.6 mmol), molecular sieves (4 Å, 2.4 g), and Ti(*i*PrO)$_4$ (370 μL, 1.25 mmol) were added to a solution of compound **18**–**21**(1.136 mmol) in dry THF (12 mL) under N_2 atmosphere. The suspension was stirred at 90 °C for ~18 h. After reaction completion, the reaction mixture was filtered through a pad of Celite and washed with THF. The solvent was evaporated under reduced pressure, and the crude was dissolved in CH_2Cl_2 (10 mL) and washed with 2 N HCl (2×10 mL). The organic layer was dried with Na_2SO_4, and the solvent was evaporated under reduced pressure.

Compound 22. The pure product was obtained after FC (CH_2Cl_2 to remove BnOH, then CH_2Cl_2/MeOH 95:5). Yield: 67%; white foam; $[\alpha]_D^{22} = -17.5$ (c = 1.00, $CHCl_3$); ^{1}H NMR (400 MHz, [D$_6$]acetone): δ = 1.30 (s, 6H, C(CH_3)$_2$ Pmc), 1.42 (s, 9H, C(CH_3)$_3$), 1.48–1.73 (m, 5H, 2*H*γ Arg, *H*β Arg *H*-7, *H*-5), 1.84 (m, 2H, CH_2CH$_2$Ar Pmc), 2.02 (m, 1H, *H*β Arg), 2.1 (s, 3H, CH_3 Pmc), 2.16 (m, 1H, *H*-8), 2.20–2.34 (m, 2H, *H*-8, *H*-7), 2.50 (m, 1H, *H*-5), 2.57 (s, 3H, CH_3 Pmc), 2.59 (s, 3H, CH_3 Pmc), 2.65 (m, 2H, CH_2CH_2Ar Pmc), 2.78 (m, 2H, 2*H*β Asp), 2.86 (m, 1H, *H*-4), 3.22 (m, 2H, 2*H*δ Arg), 3.40 (m, 1H, HC*H*O), 3.77 (m, 1H, *H*α Gly), 3.87–3.98 (m, 2H, *H*-6, HC*H*O), 4.20 (m, 1H, *H*α Gly), 4.38–4.54 (m, 3H, *H*-3, *H*-9, *H*α Arg), 4.61 (m, 1H, *H*α Asp), 5.12 (m 2H, CH_2Ph), 5.25 (m 2H, CH_2Ph), 6.18 (bs, 1H, (N*H*)$_2$C=N*H*), 6.38 (bs, 2H, (N*H*)$_2$C=N*H*), 6.56 (m, 1H, N*H* Asp), 7.12–7.30 (m, 10H, aromatic protons), 7.43–7.58 (m, 2H, N*H* Temp, N*H* Gly), 7.72 (bs, 1H, N*H* Arg); ^{13}C NMR (100.6 MHz, [D$_6$]acetone): δ = 172.0, 171.7, 171.1, 170.3, 156.4, 156.0, 152.9, 137.0, 135.7, 135.1, 135.0, 134.6, 128.5, 128.4, 128.3, 128.2, 129.7, 123.1, 117.8, 80.8, 73.4, 67.0, 66.3, 61.5, 60.5, 55.5, 52.1, 51.7, 50.8, 40.8, 40.3, 37.3, 36.3, 32.5, 31.6, 29.8, 27.3, 26.1, 26.0, 22.8, 21.1, 18.0, 16.9, 11.4; MS (ESI$^+$) *m/z*: 1003.7 [*M*+H]$^+$; Anal.: ($C_{55}H_{74}N_8O_{14}S$) C, H, N.

Compound 23. The pure product was obtained after FC (CH_2Cl_2 to remove BnOH, then CH_2Cl_2/MeOH 95:5). Yield: 90%; white foam; $[\alpha]_D^{22} = -23.4$ (c = 1.00, $CHCl_3$); ^{1}H NMR (400 MHz, [D$_6$]acetone): δ = 1.31 (s, 6H, C(CH_3)$_2$ Pmc), 1.43 (m, 9H, C(CH_3)$_3$), 1.45 (m, 1H, *H*-5), 1.51–1.70 (m, 4H, *H*-7, *H*β Arg, *H*γ Arg), 1.83 (t, 2H, J = 6.8 Hz, CH_2CH$_2$Ar Pmc), 1.86–2.00 (m, 3H, *H*-5, *H*-8, *H*β Arg), 2.10 (s, 3H, CH_3 Pmc), 2.14–2.30 (m, 2H, *H*-7, *H*-8), 2.45 (m, 1H, *H*-4), 2.58 (s, 3H, CH_3 Pmc), 2.60 (s, 3H, CH_3 Pmc), 2.63–2.70 (m, 3H, *H*β Asp, CH_2CH_2Ar Pmc), 2.87 (m, 1H, *H*β Asp), 3.18 (m, 2H, 2*H*δ Arg), 3.48 (m, 2H, CH_2OH), 3.83 (m, 1H, *H*-6), 4.02 (m, 2H, 2*H*α Gly), 4.49–4.59 (m, 2H, *H*-3, *H*α Arg), 4.60–4.68 (m, 2H, *H*-3, *H*α Asp), 5.10 (m, 2H, CH_2Ph), 5.16 (s, 2H, CH_2Ph), 6.28 (bs, 1H, (N*H*)$_2$C=N*H*), 6.60 (bs, 2H, (N*H*)$_2$C=N*H*), 6.86 (m, 1H, N*H* Arg), 7.27–7.43 (m, 10H, aromatic protons), 7.72 (m, 1H, NH scaffold), 7.86 (m, 1H, N*H* Gly), 7.97 (m, 1H, N*H* Arg); ^{13}C NMR (100.6 MHz, [D$_6$]acetone): 172.8, 172.5, 172.2, 170.6, 170.4, 169.1, 157.4, 157.0, 153.8, 138.0, 136.1, 135.9, 135.5, 129.3, 129.2, 129.0, 128.9, 128.7, 128.6, 124.0, 118.7, 81.4, 74.3, 67.1, 62.8, 61.2, 59.2, 53.1, 52.8, 51.2, 41.8, 39.8, 38.6, 33.4, 33.0, 30.0, 29.5, 28.4, 28.2, 27.0, 26.0, 22.0, 18.6, 17.8, 12.4; MS (ESI$^+$) *m/z*: 1126.1 [*M*+Na]$^+$, 1103.4 [*M*+H]$^+$; Anal.: ($C_{55}H_{74}N_8O_{14}S$) C, H, N.

Compound 24. The pure product was obtained after FC (CH_2Cl_2 to remove BnOH, then CH_2Cl_2/MeOH 95:5). Yield: 85%; white foam; $[\alpha]_D^{22} = -42.1$ (c = 1.00, $CHCl_3$); ^{1}H NMR (400 MHz, [D$_6$]acetone): δ = 1.31 (s, 6H, C(CH_3)$_2$ Pmc), 1.42 (s, 9H, C(CH_3)$_3$), 1.50–1.74 (m, 5H, 2*H*γ Arg, *H*β Arg, *H*-4, *H*-6), 1.80 (m, 1H, *H-8*), 1.83 (m, 2H, CH_2CH$_2$Ar Pmc), 1.88–1.97 (m, 3H, *H*-5, *H*-6, *H*β Arg), 1.97–2.04 (m, 2H, *H*-9, *H*-5), 2.09 (s, 3H, CH_3 Pmc), 2.11 (m, 1H, *H*-9), 2.25(m, 1H, *H*-8), 2.57 (s, 3H, CH_3 Pmc), 2.59 (s, 3H, CH_3 Pmc), 2.66 (m, 2H, CH_2CH_2Ar Pmc), 2.75 (m, 1H, *H*β Asp), 2.86 (m, 1H, *H*β Asp), 3.20 (m, 2H, 2*H*δ Arg), 3.37 (m, 1H, *H*CHO), 3.58 (m, 1H, *H*CHO), 3.72 (bs, 1H, O*H*), 3.97–4.05 (m, 2H, *H*α Gly, *H*-7), 4.10 (m, 1H, *H*α Gly), 4.50 (m, 1H, *H*-3), 4.56 (m, 2H, *H*α Arg), 4.58–4.68 (m, 2H, *H*α Asp, *H-10*), 5.12 (m, 2H, CH_2Ph), 5.18 (s, 2H, CH_2Ph), 6.18 (bs, 1H, (N*H*)$_2$C=N*H*), 6.57 (bs, 2H, (N*H*)$_2$C=N*H*), 7.05 (bs, 1H, N*H* Asp), 7.28–7.42 (m, 10H, aromatic protons), 7.70 (m, 1H, N*H* Arg), 7.86 (m, 1H, N*H* Gly), 8.06 (m, 1H, N*H* Temp); ^{13}C NMR (100.6 MHz, [D$_6$]acetone): δ = 171.9, 171.6, 170.9, 169.8, 169.5, 156.2, 152.9, 137.1, 136.1, 135.2, 134.9, 134.6, 128.5, 128.4, 128.1, 127.8, 127.7, 123.2, 117.8, 80.4, 73.4, 66.2, 63.7, 61.7, 58.7, 54.1, 52.3, 41.5, 40.9, 37.4, 33.6, 32.9, 32.5, 31.1, 29.7, 27.3, 27.2, 26.1, 21.1, 18.0, 16.9, 11.4; MS (ESI$^+$) *m/z*: 1117.4 [*M*+H]$^+$; Anal.: ($C_{56}H_{76}N_8O_{14}S$) C, H, N.

Compound 25. The pure product was obtained after FC (CH_2Cl_2 to remove BnOH, then CH_2Cl_2/MeOH 95:5). Yield: 89%; white foam; $[\alpha]_D^{22} = -21.8$ (c = 1.00, $CHCl_3$); ^{1}H NMR (400 MHz, [D$_6$]acetone): δ = 1.31 (s, 6H, C(CH_3)$_2$ Pmc), 1.43 (s, 9H, C(CH_3)$_3$), 1.50–1.68 (m, 5H, 2*H*γ Arg, *H*β Arg, *H*-4, *H*-6), 1.75 (m, 1H, *H-8*), 1.80–1.87 (m, 3H, *H*-6, CH_2CH$_2$Ar Pmc), 1.88–1.97 (m, 3H, 2*H*-5, *H*β Arg), 2.06 (m, 1H, *H*-9), 2.10 (s, 3H, CH_3 Pmc), 2.18–2.36 (m, 2H, *H*-9, *H*-8), 2.57 (s, 3H, CH_3 Pmc), 2.59 (s, 3H, CH_3 Pmc), 2.62–2.70 (m, 3H, CH_2CH_2Ar Pmc, *H*β Asp), 2.85 (m, 1H, *H*β Asp), 3.18 (m, 2H, 2*H*δ Arg), 3.47 (m, 1H, *H*CHO), 3.61 (m, 1H, *H*CHO), 3.82 (s, 1H, O*H*), 4.00 (m, 2H, 2*H*α Gly), 4.24 (m, 1H, *H*-7), 4.43 (m, 1H, *H*-3), 4.54–4.66 (m, 2H, *H*α Arg, *H-10*), 4.70 (m, 1H, *H*α Asp), 5.05–5.29 (m, 4H, 2CH_2Ph), 6.28 (bs, 1H, (N*H*)$_2$C=N*H*), 6.50 (bs, 2H, (N*H*)$_2$C=N*H*), 6.83 (m, 1H, N*H* Asp), 7.25–7.42 (m, 10H, aromatic protons), 7.53 (m, 1H, N*H* Temp), 7.62 (m, 1H, N*H* Gly), 8.07 (m, 1H, NH Arg); ^{13}C NMR (100.6 MHz, [D$_6$]acetone): δ = 172.0, 171.8, 171.5, 170.1, 169.8, 169.7, 156.4,

156.2, 152.9, 137.0, 136.1, 135.2, 135.0, 134.6, 128.4, 128.3, 128.1, 128.0, 127.8, 123.1, 117.8, 80.5, 73.4, 66.3, 63.8, 61.4, 58.7, 54.9, 52.6, 51.9, 41.3, 41.0, 40.3, 37.6, 32.8, 32.5, 32.1, 30.4, 27.3, 26.7, 26.1, 25.7, 21.1, 17.9, 16.8, 11.4; MS (ESI^+) *m/z*: 1117.7 $[M+H]^+$; Anal.: ($C_{56}H_{76}N_8O_{14}S$) C, H, N.

General procedure D: synthesis of *cyclo*-[Arg(Pmc)-Gly-Asp(*t*Bu)-Temp]. A solution of compound **22**–**25** (0.2 mmol) in MeOH (2 mL) containing a catalytic amount of 10% Pd/C was stirred overnight under H_2. After reaction completion, the mixture was filtered through a pad of Celite and washed with MeOH. The collected organic phase was evaporated under reduced pressure to yield **10**–**13** as white foam that was used without further purification. A solution of crude **10**–**13** (0.85 mmol), HATU (968 mg, 2.55 mmol), and HOAt (347 mg, 2.55 mmol) in dry DMF (251 mL), under Ar and at room temperature, was stirred for ~20 min, then dry *N*,*N*-diisopropylethylamine (DIPEA; 442 μL, 2.55 mmol) was added. The reaction mixture was stirred at 30 °C for ~4 days. After reaction completion, the solvent was evaporated, and the crude was taken up with EtOAc, washed with 5% $NaHCO_3$, and dried with Na_2SO_4. The organic phase was evaporated under reduced pressure.

Compound 26. The pure product was obtained after FC ($CHCl_3$/MeOH 9:1). Yield: 60%; white foam; $[\alpha]_D^{22} = -40.26$ (*c* = 1.17, acetone); ^{1}H NMR (400 MHz, [D$_6$]acetone): δ = 1.31 (s, 6H, C(C*H*$_3$)$_2$ Pmc), 1.43 (s, 9H, C(C*H*$_3$)$_3$), 1.48 (m, 1H, *H*-5), 1.54–1.70 (m, 3H, 2*H*γ Arg, *H*β Arg), 1.76–1.94 (m, 4H, C*H*$_2$CH$_2$Ar Pmc, *H*-7, *H*β Arg), 2.01 (m, 1H, *H*-8), 2.10 (s, 3H, C*H*$_3$ Pmc), 2.16 (m, 1H, *H*-5), 2.19–2.28 (m, 2H, *H*-8, *H*-7), 2.33 (m, 1H, *H*-4), 2.57 (s, 3H, C*H*$_3$ Pmc), 2.59 (s, 3H, C*H*$_3$ Pmc), 2.67 (m, 2H, CH$_2$C*H*$_2$Ar Pmc), 2.78 (m, 1H, *H*β Asp), 2.95 (m, 1H, *H*β Asp), 3.18–3.26 (m, 2H, 2*H*δ Arg), 3.40 (m, 1H, HC*H*O), 3.53–3.66 (m, 2H, *H*α Gly, HC*H*O), 3.76 (m, 1H, *H*-6), 3.89 (m, 1H, O*H*), 4.06 (m, 1H, *H*α Gly), 4.23 (m, 1H, *H*-9), 4.48 (m, 1H, *H*α Arg), 4.63–4.80 (m, 2H, *H*α Asp, *H*-3), 6.41 (bs, 1H, (N*H*)$_2$C=N*H*), 6.42 (bs, 2H, (N*H*)$_2$C=N*H*), 6.90 (bs, 1H, N*H* Arg), 7.80 (bs, 1H, N*H* Temp), 8.10 (bs, 1H, N*H* Asp), 8.63 (bs, 1H, NH Gly); ^{13}C NMR (100.6 MHz, [D$_6$]acetone): δ = 174.6, 172.9, 172.7, 170.2, 169.8, 167.4 156.5 152.9, 135.2, 134.8, 134.6, 123.2, 117.8, 80.9, 73.4, 62.1, 61.8, 60.4, 51.3, 50.8, 50.1, 45.0, 42.7, 40.0, 36.9, 32.5, 31.3, 27.8, 27.4, 26.1, 25.6, 21.1, 18.0, 16.9, 11.4; MS (ESI^+) *m/z*: 861.5 $[M+H]^+$; Anal.: ($C_{40}H_{60}N_8O_{11}S$) C, H, N.

Compound 27. The pure product was obtained after reversed-phase column chromatography on a Biotage C_{18} 25+M cartridge eluting with H_2O/MeCN (90:10→10:90). Yield: 54%; white foam; $[\alpha]_D^{22} = -62.86$ (*c* = 1.05, acetone); ^{1}H NMR (400 MHz, [D$_6$]acetone): δ = 1.32 (s, 6H, C(C*H*$_3$)$_2$ Pmc), 1.43 (s, 9H, C(C*H*$_3$)$_3$), 1.45–1.62 (m, 4H, 2*H*γ Arg, *H*β Arg, *H*-5), 1.68 (m, 1H, *H*-7), 1.85 (t, 2H, *J* = 6.8 Hz, C*H*$_2$CH$_2$, Ar Pmc), 1.98 (m, 1H, *H*-8), 2.10 (s, 3H, C*H*$_3$ Pmc), 2.11 (m, 1H, *H*β Arg), 2.30–2.49 (m, 3H, *H*-5, *H*-8, *H*-7), 2.56 (m, 1H, *H*β Asp), 2.57 (s, 3H, C*H*$_3$ Pmc), 2.59 (s, 3H, C*H*$_3$ Pmc), 2.63 (m, 1H, *H*-4), 2.67 (m, 2H, CH$_2$C*H*$_2$Ar Pmc), 3.00 (dd, 1H, *J* = 7.2 Hz, *J* = 16.6 Hz, *H*β Asp), 3.21 (m, 2H, 2*H*δ Arg), 3.38 (d, 1H, *J* = 13.9 Hz, *H*α Gly), 3.44 (m, 1H, HC*H*O), 3.53 (m, 1H, HC*H*O), 3.62 (bs, 1H, O*H*), 4.17 (m, 1H, *H*-6), 4.19 4.30 (m, 3H, *H*-9, *H*α Gly, *H*-3), 4.50–4.61 (m, 2H, *H*α Arg, *H*α Asp), 6.28 (bs, 1H, (N*H*)$_2$C=N*H*), 6.47 (bs, 2H, (N*H*)$_2$C=N*H*), 7.18 (d, 1H, *J* = 4.9 Hz, N*H* Temp), 7.38 (d 1H, *J* = 9.0 Hz, N*H* Arg), 7.62 (d, 1H, *J* = 8.7 Hz, N*H* Gly), 8.20 (d, 1H, *J* = 7.8 Hz, NH Asp); ^{13}C NMR (100.6 MHz, [D$_6$]acetone): δ = 174.2, 172.4, 171.4, 171.1, 171.0, 157.3, 153.8, 136.0, 135.8, 135.5, 124.0, 118.7, 80.9, 74.2, 63.3, 62.0, 56.6, 53.7, 52.3, 51.9, 43.7, 41.2, 39.0, 35.8, 34.1, 33.3, 33.0, 30.9, 29.0, 28.2, 27.0, 26.9, 21.9, 18.8, 17.7, 12.3; MS (ESI^+) *m/z*: 861.7 $[M+H]^+$; Anal.: ($C_{40}H_{60}N_8O_{11}S$) C, H, N.

Compound 28. The pure product was obtained after reversed-phase column chromatography on a Biotage C_{18} 25+M cartridge eluting with H_2O/MeCN (90:10→10:90). Yield: 60%; white foam; $[\alpha]_D^{22} = -56.2$ (*c* = 1.00, $CHCl_3$); ^{1}H NMR (600 MHz, [D$_6$]acetone): δ = 1.32 (s, 6H, C(C*H*$_3$)$_2$ Pmc), 1.45 (s, 9H, C(C*H*$_3$)$_3$), 1.50–1.68 (m, 3H, 2*H*γ Arg, *H*β Arg), 1.74–1.86 (m, 6H, *H*-5, *H*-6, *H*-8, *H*β Arg, C*H*$_2$CH$_2$Ar Pmc), 1.86–1.97 (m, 2H, *H*-5, *H*-9), 2.06 (m, 1H, *H*-4), 2.10 (s, 1H, C*H*$_3$ Pmc), 2.13 (m, 1H, *H*-9), 2.20 (m, 1H, *H*-6), 2.30 (m, 1H, *H*-8), 2.57 (s, 3H, C*H*$_3$ Pmc), 2.59 (s, 3H, C*H*$_3$ Pmc), 2.67 (m, 2H, CH$_2$C*H*$_2$Ar Pmc), 2.80 (m, 1H, *H*β Asp), 2.88 (m, 1H, *H*β Asp), 3.20–3.32 (m, 2H, 2*H*δ Arg), 3.53 (m, 1H, *H*CHO), 3.62 (m, 1H, *H*α Gly), 3.70 (m, 1H, *H*CHO), 3.89 (bs, 1H, *H*-7), 3.97 (m, 1H, *H*α Gly), 4.15 (m, 1H, *H*-10), 4.44 (m, 1H, *H*-3), 4.52 (m, 1H, *H*α Arg), 4.83 (m, 1H, *H*α Asp), 6.37 (bs, 1H, (N*H*)$_2$C=N*H*), 6.56 (bs, 2H, (N*H*)$_2$C=N*H*), 6.77 (m, 1H, N*H* Arg), 7.75 (m, 1H, N*H* Temp), 8.17 (m, 1H, NH Asp), 8.76 (m, 1H, N*H* Gly); ^{13}C NMR (150.95 MHz, [D$_6$]acetone): δ = 174.5, 173.2, 170.7, 170.6, 170.1, 156.5, 152.9, 135.2, 134.7, 123.2, 117.8, 80.7, 73.4, 66.3, 65.7, 59.7, 56.5, 52.3, 50.8, 44.9, 42.9, 36.1, 34.5, 32.9, 32.5, 31.6, 27.4, 26.5, 26.1, 21.1, 18.1, 16.9, 11.5; MS (ESI^+) *m/z*: 875.5 $[M+H]^+$; Anal.: ($C_{41}H_{62}N_8O_{11}S$) C, H, N.

Compound 29. The pure product was obtained after FC ($CHCl_3$/MeOH 9:1). Yield: 74%; white foam; $[\alpha]_D^{22} = -27.2$ (*c* = 1.00, $CHCl_3$); ^{1}H NMR (400 MHz, [D$_6$]acetone): δ = 1.32 (s, 6H, C(C*H*$_3$)$_2$ Pmc), 1.45 (s, 9H, C(C*H*$_3$)$_3$), 1.46–1.68 (m, 5H, 2*H*γ Arg, *H*β Arg, *H*-4, *H*-6), 1.75–1.90 (m, 4H, *H*-6, *H*-8, C*H*$_2$CH$_2$Ar Pmc), 1.90–2.03 (m, 2H, *H*-5, *H*-9), 2.03–2.14 (m, 5H, *H*β Arg, *H*-5, C*H*$_3$ Pmc), 2.26–2.44 (m, 2H, *H*-9, *H*-8), 2.55 (m, 1H, *H*β Asp), 2.57 (s, 3H, C*H*$_3$ Pmc), 2.59 (s, 3H, C*H*$_3$ Pmc), 2.68 (m, 2H, CH$_2$C*H*$_2$Ar Pmc), 2.92 (m, 1H, *H*β Asp), 3.12–3.28 (m, 2H, 2*H*δ Arg), 3.31–3.43 (m, 2H, *H*CHO, *H*α Gly), 3.75 (m, 1H, *H*CHO), 3.90 (bs, 1H, O*H*), 4.20–4.35 (m, 2H, *H*-7, *H*α Gly), 4.40–4.55 (m, 3H, *H*-10, *H*-3, *H*α Arg), 5.87 (m, 1H, *H*α Asp), 6.38 (bs, 1H, (N*H*)$_2$C=N*H*), 6.50 (bs, 2H, (N*H*)$_2$C=N*H*), 7.28 (m, 1H, N*H* Gly), 7.52 (m, 1H, N*H* Arg), 7.72 (d, 1H, *J* = 6.4 Hz, N*H* Temp), 8.16 (d, 1H, *J* = 8.3 Hz, NH Asp); ^{13}C NMR (100.6 MHz, [D$_6$]acetone): δ = 173.5, 172.4, 171.3, 169.8, 169.7, 156.4, 152.9, 135.1, 134.9, 134.6, 123.1, 117.8, 80.1, 73.4, 63.8, 63.2, 59.3, 55.4, 51.7, 49.9, 43.4, 41.2, 40.4, 35.0, 33.1, 32.5, 32.2, 30.6, 27.9, 27.6, 27.3, 26.1, 26.0, 21.1, 17.9, 16.8, 11.4; MS (ESI^+) *m/z*: 875.3 $[M+H]^+$; Anal.: ($C_{41}H_{62}N_8O_{11}S$) C, H, N.

General procedure E: synthesis of azide derivatives 34–**37**. MsCl (80 μL, 1.02 mmol) and TEA (280 μL, 2.04 mmol) were added to a solution of compound **26**–**29** (0.51 mmol) in dry CH_2Cl_2 (5.1 mL) under N_2 at room temperature. The solution was stirred for ~1 h, then a saturated solution of NH_4Cl was added, and the intermediate was extracted with CH_2Cl_2. The organic phase, dried with Na_2SO_4, was evaporated under reduced pressure. The crude was dissolved in dry DMF (5.1 mL) and, under N_2 at room temperature, NaN_3 (330 mg, 5.1 mmol) was added. The reaction was stirred at 80 °C for ~18 h. After reaction completion, the resulting suspension was filtered through a pad of Celite and washed with CH_2Cl_2. The combined filtrates were evaporated under reduced pressure. The crude was purified by FC.

Compound 34. The pure product was obtained after FC (CH_2Cl_2/*i*PrOH 9:1→8:2). Yield: 62%; white solid; $[\alpha]_D^{22} = -6.3$ (*c* = 1.00, $CHCl_3$); ^{1}H NMR (400 MHz, [D$_6$]acetone): δ = 1.33 (s, 6H, C(C*H*$_3$)$_2$ Pmc), 1.47 (s, 9H, C(C*H*$_3$)$_3$), 1.52–1.69 (m, 4H, 2*H*γ Arg, *H*β Arg, *H*-5), 1.77–1.92 (m, 4H, *H*-7, *H*β Arg, C*H*$_2$CH$_2$Ar Pmc), 1.97 (m, 1H, *H*-8), 2.11 (s, 3H, C*H*$_3$ Pmc), 2.13–2.20 (m, 2H, *H*-7, *H*-8), 2.24 (m, 1H, *H*-5), 2.42 (m, 1H, *H*-4), 2.58 (s, 3H, C*H*$_3$ Pmc), 2.60 (s, 3H, C*H*$_3$ Pmc), 2.68 (m, 2H, CH$_2$C*H*$_2$Ar Pmc), 2.74 (m, 1H, *H*β Asp), 2.92 (dd, 1H, *J* = 6.6 Hz, *J* = 16.6 Hz, *H*β Asp), 3.28–3.40 (m, 3H, 2*H*δ Arg, HC*H*N$_3$), 3.47 (d, 1H, *J* = 14.0 Hz, *H*α Gly), 3.61 (m, 1H, HC*H*N$_3$), 3.73 (m, 1H, *H*-6), 4.09 (d, 1H, *J* = 14.0 Hz, *H*α Gly), 4.18 (d, 1H, *J* = 9.2 Hz, *H*-9),

4.39 (m, 1H, *H*α Arg), 4.66–4.80 (m, 2H, *H*-3, *H*α Asp), 6.40 (bs, 1H, (N*H*)$_2$C=N*H*), 6.52 (bs, 2H, (N*H*)$_2$C=N*H*), 6.90 (bs, 1H, N*H* Arg), 7.64 (m, 1H, N*H* Asp), 7.70 (m, 1H, N*H* Temp), 8.52 (bs, 1H, N*H* Gly); ^{13}C NMR (100.6 MHz, [D$_6$]acetone): δ = 174.5, 172.3, 171.4, 170.5, 168.9, 166.5, 156.5, 152.9, 135.2, 134.6, 123.1, 117.8, 80.7, 73.4, 61.7, 59.7, 52.3, 51.2, 50.3, 49.6, 45.0, 39.9, 39.6, 37.1, 32.5, 31.3, 31.1, 27.4, 26.1, 25.6, 21.1, 17.9, 16.8, 11.4; MS (ESI$^+$) *m/z*: 886.6 [*M*+H]$^+$; Anal.: (C$_{40}$H$_{59}$N$_{11}$O$_{10}$S) C, H, N.

Compound 35. The pure product was obtained after FC (CH$_2$Cl$_2$/MeOH 95:5→9:1). Yield: 90%; white solid; $[\alpha]_D^{22} = -65.83$ (*c* = 1.15, CHCl$_3$); ^{1}H NMR (400 MHz, [D$_6$]acetone): δ = 1.32 (s, 6H, C(C*H*$_3$)$_2$ Pmc), 1.36 (m, 1H, *H*-5), 1.45 (s, 9H, C(C*H*$_3$)$_3$), 1.47–1.56 (m, 2H, *H*γ Arg, *H*β Arg), 1.59 (m, 1H, *H*γ Arg), 1.68 (m, 1H, *H*-7), 1.85 (t, 2H, *J* = 6.8 Hz, C*H*$_2$CH$_2$, Ar Pmc), 1.96–2.08 (m, 2H, *H*-8, *H*β Arg), 2.10 (s, 3H, C*H*$_3$ Pmc), 2.36–2.50 (m, 3H, *H*-5, *H*-8, *H*-7), 2.54–2.64 (m, 7H, *H*β Asp, 2C*H*$_3$ Pmc), 2.67 (t, 2H, *J* = 6.8 Hz, CH$_2$C*H*$_2$Ar Pmc), 2.88 (m, 1H, *H*-4), 3.02 (dd, 1H, *J* = 6.8 Hz, *J* = 16.4 Hz, *H*β Asp), 3.21 (m, 2H, 2*H*δ Arg), 3.37 (dd, 1H, *J* = 5.8 Hz, *J* = 12.2 Hz, HC*H*N$_3$), 3.42–3.51 (m, 2H, *H*α Gly, HC*H*N$_3$), 4.14–4.32 (m, 4H, *H*-6, *H*-3, *H*α Gly, *H*-9), 4.50–4.621 (m, 2H, *H*α Arg, *H*α Asp), 6.38 (bs, 1H, (N*H*)$_2$C=N*H*), 6.51 (bs, 2H, (N*H*)$_2$C=N*H*), 7.34 (d, 1H, *J* = 3.6 Hz, N*H* Temp), 7.47 (d 1H, *J* = 9.2 Hz, N*H* Arg), 7.61 (d, 1H, *J* = 8.0 Hz, N*H* Gly), 8.44 (d, 1H, *J* = 7.6 Hz, NH Asp); ^{13}C NMR (100.6 MHz, [D$_6$]acetone): δ = 173.7, 171.6, 171.4, 170.2, 170.0, 169.2, 156.4, 152.9, 135.1, 134.9 134.6, 123.1, 117.8, 80.0, 73.4, 62.6, 59.5, 55.6, 53.0, 52.6, 51.6, 51.2, 42.7, 40.5, 35.8, 34.9, 33.2, 33.0, 32.5, 29.9, 27.4, 26.1, 21.1, 17.9, 16.8, 11.4; MS (ESI$^+$) *m/z*: 886.4 [*M*+H]$^+$; Anal.: (C$_{40}$H$_{59}$N$_{11}$O$_{10}$S) C, H, N.

Compound 36. The pure product was obtained after reversed-phase column chromatography on a Biotage C$_{18}$ 25+M cartridge eluting with H$_2$O/MeCN (90:10→10:90). Yield: 83%; white foam; $[\alpha]_D^{22} = -65.2$ (*c* = 1.00, CHCl$_3$); ^{1}H NMR (600 MHz, [D$_6$]acetone): δ = 1.32 (s, 6H, C(CH$_3$)$_2$ Pmc), 1.46 (s, 9H, C(CH$_3$)$_3$), 1.49–1.70 (m, 3H, 2*H*γ Arg, *H*β Arg), 1.72–1.96 (m, 8H, *H*β Arg, 2*H*-5, *H*-6, *H*-8, *H*-9, C*H*$_2$CH$_2$Ar Pmc), 2.09–2.22 (m, 5H, C*H*$_3$ Pmc, *H*-9, *H*-6), 2.27–2.38 (m, 2H, *H*-4 *H*-8), 2.57 (s, 3H, C*H*$_3$ Pmc), 2.59 (s, 3H, C*H*$_3$ Pmc), 2.67 (m, 2H, CH$_2$C*H*$_2$Ar Pmc), 2.78–2.98 (m, 2H, *H*β Asp), 3.20–3.30 (m, 2H, 2*H*δ Arg), 3.53 (m, 1H, *H*CHN$_3$), 3.60 (m, 1H, *H*α Gly), 3.69 (m, 1H, *H*CHN$_3$), 3.90 (m, 1H, *H*-7), 3.99 (m, 1H, *H*α Gly), 4.18 (m, 1H, *H*-10), 4.47 (m, 1H, *H*-3), 4.53 (m, 1H, *H*α Arg), 4.80 (m, 1H, *H*α Asp), 6.40 (bs, 1H, (N*H*)$_2$C=N*H*), 6.54 (bs, 2H, (N*H*)$_2$C=N*H*), 6.72 (m, 1H, N*H* Arg), 7.63 (m, 1H, N*H* Temp), 8.18 (m, 1H, NH Asp), 8.75 (m, 1H, N*H* Gly); ^{13}C NMR (150.95 MHz, [D$_6$]acetone): δ = 174.4, 173.1, 172.5, 170.4, 170.1, 156.5, 152.9, 135.2, 134.9, 134.7, 123.1, 117.8, 80.7, 73.4, 66.2, 59.4, 56.5, 56.0, 52.3, 51.1, 44.7, 40.4, 36.4, 34.2, 32.9, 32.6, 31.9, 29.7, 27.4, 26.1, 21.1, 18.1, 16.9, 11.5; MS (ESI$^+$) *m/z*: 900.9 [*M*+H]$^+$; Anal.: (C$_{41}$H$_{61}$N$_{11}$O$_{10}$S) C, H, N.

Compound 37. The pure product was obtained after FC (CH$_2$Cl$_2$/*i*PrOH 9:1→8:2). Yield: 75%; white solid; $[\alpha]_D^{22} = -35.74$ (*c* = 1.20, CHCl$_3$); ^{1}H NMR (400 MHz, [D$_6$]acetone): δ = 1.32 (s, 6H, C(C*H*$_3$)$_2$ Pmc), 1.40–1.52 (m, 11H, C(C*H*$_3$)$_3$, *H*β Arg, *H*γ Arg), 1.53–1.76 (m, 4H, *H*γ Arg, *H*-6, *H*-5, *H*-4), 1.80 (m, 1H, *H*-8), 1.85 (m, 2H, C*H*$_2$CH$_2$Ar Pmc),1.91 (m, 1H, *H*-6), 1.99 (m, 1H, *H*-9), 2.06 (m, 1H, *H*β Arg), 2.10 (s, 3H, C*H*$_3$ Pmc), 2.13 (m, 1H, *H*-5), 2.28–2.33 (m, 2H, *H*-8, *H*-9), 2.53 (m, 1H, *H*β Asp), 2.56 (s, 3H, C*H*$_3$ Pmc), 2.58 (s, 3H, C*H*$_3$ Pmc), 2.68 (m, 2H, CH$_2$C*H*$_2$Ar Pmc), 2.88 (m, 1H, *H*β Asp), 3.16–3.28 (m, 3H, 2*H*δ Arg, *H*CHN$_3$), 3.46 (d, 1H, *J* = 13.9 Hz, *H*α Gly), 3.72 (m, 1H, *H*CHN$_3$), 4.21–3.36 (m, 2H, *H*-7, *H*α Gly), 4.39–4.52 (m, 3H, *H*-10, *H*-3, *H*α Arg), 4.82 (m, 1H, *H*α Asp), 6.31 (bs, 1H, (N*H*)$_2$C=N*H*), 6.49 (bs, 2H, (N*H*)$_2$C=N*H*), 7.30 (d, 1H, *J* = 8.0 Hz, N*H* Gly), 7.40–7.50 (m, 2H, N*H* Arg, N*H* Temp), 7.92 (d, 1H, *J* = 8.7 Hz, N*H* Asp); ^{13}C NMR (100.6 MHz, [D$_6$]acetone): δ = 171.4, 171.3, 169.8, 169.6, 156.4, 152.9, 135.1, 134.6, 123.1, 117.8, 80.1, 73.4, 63.2, 59.1, 55.2, 54.0, 51.7, 49.8, 43.6, 40.4, 39.5, 34.9, 32.5, 32.2, 31.3, 28.0, 27.6, 27.4, 26.1, 26.0, 21.1, 17.9, 16.8, 11.4; MS (ESI$^+$) *m/z*: 900.4 [*M*+H]$^+$; Anal.: (C$_{41}$H$_{61}$N$_{11}$O$_{10}$S) C, H, N.

General procedure F: synthesis of the amide derivatives 38–40. Catalytic 10% Pd/C was added to a solution of compound **34**, **35**, or **37** (0.27 mmol) in MeOH (10 mL). The suspension was stirred under H$_2$ for ~18 h. After this time, the catalyst was filtered through a pad of Celite and washed with MeOH. The collected organic phase was evaporated under reduced pressure to yield the desired compound as a white foam, which was used without further purification. Valeroyl chloride (6.5 μL, 0.054 mmol) and TEA (15 μL, 0.11 mmol) were added to a solution of the crude (0.027 mmol) in dry CH$_2$Cl$_2$ (700 μL) under N$_2$ at room temperature. The solution was stirred for ~1.5 h. After this time, the solvent was evaporated, and the crude was purified by FC to yield the desired product.

Compound 38. The pure product was obtained after FC (CH$_2$Cl$_2$/*i*PrOH 85:15→8:2). Yield: 40%; white solid; $[\alpha]_D^{22} = -83.10$ (*c* = 0.48, acetone); ^{1}H NMR (400 MHz, [D$_6$]acetone): δ = 0.9 (t, 3H, *J* = 7.4 Hz, COCH$_2$CH$_2$CH$_2$C*H*$_3$), 1.22–1.39 (m, 8H, C(C*H*$_3$)$_2$ Pmc, COCH$_2$CH$_2$C*H*$_2$CH$_3$), 1.45 (s, 9H, C(C*H*$_3$)$_3$), 1.50–1.75 (m, 7H, 2*H*γ Arg, COCH$_2$C*H*$_2$CH$_2$CH$_3$, 2*H*-5, *H*β Arg), 1.75–2.0 (m, 5H, *H*-7, C*H*$_2$CH$_2$Ar Pmc, *H*β Arg, *H*-8), 2.10 (s, 3H, C*H*$_3$ Pmc), 2.12–2.32 (m, 5H, COC*H*$_2$CH$_2$CH$_2$CH$_3$, *H*-7, *H*-8, *H*-4), 2.57 (s, 3H, C*H*$_3$ Pmc), 2.59 (s, 3H, C*H*$_3$ Pmc), 2.67 (m, 2H, CH$_2$C*H*$_2$Ar Pmc), 2.78(m, 1H, *H*β Asp), 2.88–3.00 (m, 2H, *H*CHNHCO, *H*β Asp), 3.27 (m, 2H, 2*H*δ Arg), 3.48 (m, 1H, *H*α Gly), 3.57 (m, 1H, *H*CHNHCO), 3.69 (m, 1H, *H*-6), 4.08–4.22 (m, 2H, *H*α Gly, *H*-9), 4.43 (m, 1H, *H*α Arg), 4.62 (m, 1H, *H*-3), 4.8 (m, 1H, *H*α Asp), 6.5 (m, 3H, (N*H*)$_2$C=N*H*), 7.08 (m, 1H, N*H*CO-(CH$_2$)$_3$CH$_3$), 7.12 (bs, 1H, N*H* Arg), 7.88 (m, 1H, N*H* Asp), 8.0 (bs, 1H, N*H* Temp), 8.4 (bs, 1H, N*H* Gly); ^{13}C NMR HETCOR (400 MHz, [D$_6$]acetone): δ = 61.9, 60.5, 51.7, 51.3, 50.5, 45.1, 40.5, 40.4, 40.1, 37.7, 36.4, 32.9, 31.7, 30.8, 30.7, 28.2, 28.0, 27.6, 26.4, 25.9, 22.5, 21.6, 18.6, 17.1, 16.6, 11.8; MS (ESI$^+$) *m/z*: 944.5 [*M*+H]$^+$; Anal.: (C$_{45}$H$_{69}$N$_9$O$_{11}$S) C, H, N.

Compound 39. The pure product was obtained after FC (CH$_2$Cl$_2$/*i*PrOH 8:2). Yield: 54%; white solid; $[\alpha]_D^{22} = -84.4$ (*c* = 0.75, acetone); ^{1}H NMR (400 MHz, [D$_6$]acetone): δ = 0.9 (t, 3H, *J* = 7.3 Hz, COCH$_2$CH$_2$CH$_2$C*H*$_3$), 1.25–1.40 (m, 9H, COCH$_2$CH$_2$C*H*$_2$CH$_3$, C(C*H*$_3$)$_2$ Pmc, *H*-5), 1.45 (s, 9H, C(C*H*$_3$)$_3$), 1.48–1.70 (m, 6H, 2*H*γ Arg, *H*β Arg, COCH$_2$C*H*$_2$CH$_2$CH$_3$, *H*-7), 1.85 (m, 2H, C*H*$_2$CH$_2$Ar Pmc), 2.0 (m, 1H, *H*-8), 2.08 (m, 1H, *H*β Arg), 2.1 (s, 3H, C*H*$_3$ Pmc), 2.12 (m, 2H, COC*H*$_2$CH$_2$CH$_2$CH$_3$), 2.35–2.50 (m, 3H, *H*-7, *H*-8, *H*-5), 2.56 (m, 1H, *H*β Asp), 2.57 (s, 3H, C*H*$_3$ Pmc), 2.59 (s, 3H, C*H*$_3$ Pmc), 2.68 (m, 2H, CH$_2$C*H*$_2$Ar Pmc), 2.74 (m, 1H, *H*-4), 3.01 (dd, 1H, *J* = 16.6 Hz, *J* = 7.0 Hz, *H*β Asp), 3.12 (m, 1H, *H*CHNHCO), 3.15–3.26 (m, 3H, *H*CHNHCO, 2*H*δ Arg), 3.43 (d, 1H, *J* = 14.2 Hz, *H*α Gly), 4.13–4.36 (m, 4H, *H*-6, *H*α Gly, *H*-9, *H*-3), 4.50–4.62 (m, 2H, *H*α Arg, *H*α Asp), 6.32 (bs, 1H, (N*H*)$_2$C=N*H*), 6.48 (bs, 2H, (N*H*)$_2$C=N*H*), 6.67 (m, 1H, N*H*CO(CH$_2$)$_3$CH$_3$), 7.33 (m, 1H, N*H* Temp), 7.42 (m, 1H, N*H* Arg), 7.58 (m, 1H, N*H* Gly), 8.32 (m, 1H, N*H* Asp); ^{13}C NMR HETCOR (400 MHz, [D$_6$]acetone): δ = 62.5, 55.7, 53.4, 51.2, 42.7, 40.6, 40.3, 36.3, 35.5, 34.9, 33.4, 33.3, 33.4, 30.0, 28.4, 28.3, 27.5, 26.0, 22.1, 20.8, 17.9, 16.7, 13.2, 11.4; MS (ESI$^+$) *m/z*: 944.6 [*M*+H]$^+$; Anal.: (C$_{45}$H$_{69}$N$_9$O$_{11}$S) C, H, N.

Compound 40. The pure product was obtained after FC (CH$_2$Cl$_2$/*i*PrOH 85:15). Yield: 57%; white solid; $[\alpha]_D^{22} = -13.78$ (*c* = 1.02, acetone); ^{1}H NMR (400 MHz, [D$_6$]acetone): δ = 0.92 (t, 3H, *J* = 7.4 Hz, COCH$_2$CH$_2$CH$_2$C*H*$_3$), 1.32 (s, 6H, C(C*H*$_3$)$_2$ Pmc), 1.34 (m, 2H, COCH$_2$CH$_2$C*H*$_2$CH$_3$), 1.45 (s, 9H, C(C*H*$_3$)$_3$), 1.46–1.53 (m, 2H, *H*γ Arg, *H*β Arg), 1.52–1.63 (m, 4H, *H*γ Arg, COCH$_2$C*H*$_2$CH$_2$CH$_3$, *H*-6), 1.63–

1.73 (m, 2H, *H*-5, *H*-4), 1.73–1.89 (m, 4H, *H*-8, CH_2CH_2Ar Pmc, *H*-6), 1.90–2.01 (m, 2H, *H*-5, *H*-9), 2.06 (m, 1H, *H*β Arg), 2.1 (s, 3H, CH_3 Pmc), 2.12 (m, 2H, $COCH_2CH_2CH_2CH_3$), 2.22–2.43 (m, 2H, *H*-8, *H*-9), 2.54 (m, 1H, *H*β Asp), 2.56 (s, 3H, CH_3 Pmc), 2.58 (s, 3H, CH_3 Pmc), 2.67 (m, 2H, CH_2CH_2Ar Pmc), 2.94 (m, 1H, *H*β Asp), 3.05 (m, 1H, *H*CHNHCO), 3.20 (m, 2H, 2*H*δ Arg), 3.37 (d, 1H, $J=14.3$ Hz, *H*α Gly), 3.65 (m, 1H, *H*CHNHCO), 4.20–4.34 (m, 2H, *H*-7, *H*α Gly), 4.36–4.54 (m, 3H, *H*-3, *H*-10, *H*α Arg), 4.85 (m, 1H, *H*α Asp), 6.33 (bs, 1H, $(NH)_2C{=}NH$), 6.48 (bs, 2H, $(NH)_2C{=}NH$), 7.13 (m, 1H, NHCO-$(CH_2)_3CH_3$), 7.27 (m, 1H, N*H* Gly), 7.48 (m, 1H, N*H* Arg) 7.61 (m, 1H, N*H* Temp), 8.04 (m, 1H, N*H* Asp); ^{13}C NMR HETCOR (400 MHz, [D$_6$]acetone): $\delta=63.1$, 59.2, 55.7, 51.7, 49.9, 43.6, 40.8, 40.3, 39.6, 35.9, 34.8, 33.0, 32.6, 32.2, 31.4, 27.8, 27.7, 27.5, 27.3, 26.1, 26.0, 22.1, 21.0, 17.9, 16.9, 13.3, 11.4; MS (ESI$^+$) *m/z*: 958.7 $[M+H]^+$; Anal.: ($C_{46}H_{71}N_9O_{11}S$) C, H, N.

General procedure G: synthesis of the ester derivative 41. Pyridine (22 μL, 22.0 mg, 0.275 mmol, 5 equiv) and a catalytic amount of 4-dimethylaminopyridine (DMAP) were added to a solution of compound **28** (48 mg, 0.055 mmol) in dry THF (1.0 mL) under Ar. Valeroyl chloride (10 μL, 9.92 mg, 0.822 mmol, 1.5 equiv) was added dropwise to this solution. The resulting mixture was left to stir at room temperature for 24 h. After 24 h, further amounts of pyridine (22 μL, 22.0 mg, 0.275 mmol, 5 equiv) and valeroyl chloride (10 μL, 9.92 mg, 0.822 mmol, 1.5 equiv) were added, and the solution was left to stir for 24 h. After 48 h the reaction was quenched with H_2O and then purified by reversed-phase column chromatography on a Biotage 25+M cartridge, eluting with H_2O/MeCN (90:10→10:90) to give the desired compound.

Compound 41. Yield: 84%; white solid; $[\alpha]_D^{22}=-53.80$ ($c=0.90$, $CHCl_3$); ^{1}H NMR (600 MHz, [D$_6$]acetone): $\delta=0.92$ (t, 3H, $J=7.3$ Hz, $COCH_2CH_2CH_2CH_3$), 1.32 (s, 6H, $C(CH_3)_2$ Pmc), 1.36 (m, 2H, $COCH_2CH_2CH_2CH_3$) 1.43 (s, 9H, $C(CH_3)_3$), 1.50–1.68 (m, 5H, 2*H*γ Arg, *H*β Arg, $COCH_2CH_2CH_2CH_3$), 1.77 (m, 1H, *H*β Arg), 1.80–1.88 (m, 6H, *H*-5, *H*-6, *H*-8, *H*-9, CH_2CH_2Ar Pmc), 1.93 (m, 1H, *H*-5), 2.10 (s, 3H, CH_3 Pmc), 2.11(m, 1H, *H*-9), 2.18 (m, 1H, *H*-8), 2.30 (m, 2H, $COCH_2CH_2CH_2CH_3$), 2.42 (m, 1H, *H*-4), 2.58 (s, 3H, CH_3 Pmc), 2.60 (s, 3H, CH_3 Pmc), 2.62–2.70 (m, 3H, CH_2CH_2Ar Pmc, *H*β Asp), 2.68 (m, 1H, *H*β Asp), 3.20–3.33 (m, 2H, 2*H*δ Arg), 3.56 (m, 1H, *H*α Gly), 3.89–3.97 (m, 2H, *H*-7, *H*CHO), 4.02 (m, 1H, *H*α Gly), 4.15 (m, 1H, *H*-10), 4.40 (dd, 1H, $J=10.9$ Hz, $J=5.3$ Hz, *H*CHO), 4.45–4.53(m, 2H, *H*-3, *H*α Arg), 4.79 (m, 1H, *H*α Asp), 6.37 (bs, 1H, $(NH)_2C{=}NH$), 6.48 (bs, 2H, $(NH)_2C{=}NH$), 6.65 (m, 1H, N*H* Arg), 7.57 (m, 1H, N*H* Temp), 8.12 (m, 1H, NH Asp), 8.62 (bs, 1H, N*H* Gly); ^{13}C NMR (150.95 MHz, [D$_6$]acetone): $\delta=174.4$, 172.8, 172.7, 170.2, 170.0, 156.5, 152.9, 135.2, 134.6, 123.1, 100.0, 80.4, 73.4, 67.3, 66.2, 59.4, 55.8, 52.3, 51.4, 44.6, 39.8, 36.7, 34.4, 33.5, 32.9, 32.6, 31.9, 29.8, 27.4, 26.8, 26.6, 26.1, 22.1, 21.1, 18.1, 16.9, 13.2, 11.5; MS (ESI$^+$) *m/z*: 959.5 $[M+H]^+$; Anal.: ($C_{46}H_{70}N_8O_{12}S$) C, H, N.

General procedure H: deprotection reaction. A solution of protected compound (0.015 mmol) in TFA/thioanisole/1,2-ethanedithiol/anisole (90:5:3:2; 1 mL) was stirred at room temperature for 2 h. The solvent was evaporated under reduced pressure, and then the crude was dissolved in H_2O and washed with iPr_2O. The aqueous phase was evaporated under reduced pressure, and the crude was purified by HPLC.

Compound 30. Yield: 93%; white foam; $[\alpha]_D^{22}=-59.08$ ($c=1.02$, MeOH); ^{1}H NMR (400 MHz, D$_2$O): $\delta=1.33$ (m, 1H, *H*-5), 1.41–1.62 (m, 3H, 2*H*γ Arg, *H*β Arg), 1.62–1.80 (m, 2H, *H*-7, *H*β Arg), 1.90 (m, 1H, *H*-8), 2.12–2.24 (m, 3H, *H*-8, *H*-7, *H*-5), 2.28 (m, 1H, *H*-4), 2.78–2.92 (m, 2H, 2*H*β Asp), 3.03–3.18 (m, 2H, 2*H*δ Arg), 3.37 (dd, 1H, $J=7.4$ Hz, $J=11.3$ Hz, HC*H*O), 3.47–3.57 (m, 2H, *H*α Gly, HC*H*O), 3.63 (m, 1H, *H*-6), 3.94 (d, 1H, $J=14.2$ Hz, *H*α Gly), 4.17–4.27 (m, 2H, *H*-9, *H*α Arg), 4.61 (dd, 1H, $J=5.2$ Hz, $J=7.2$ Hz, *H*α Asp), 4.67(m, 1H, *H*-3); ^{13}C NMR HETCOR (400 MHz, D$_2$O): $\delta=62.2$, 62.0, 60.9, 52.2, 51.8, 49.8, 45.1, 40.8, 40.9, 40.8, 36.0, 31.2, 29.9, 29.0, 28.3, 24.8; for a more detailed NMR characterization, see the Supporting Information; MS (ESI$^+$) *m/z*: 539.5 $[M+H]^+$; Anal.: ($C_{22}H_{34}N_8O_8{\cdot}CF_3CO_2H$) C, H, N.

Compound 31. Yield: 85%; white foam; $[\alpha]_D^{22}=-49.9$ ($c=1.00$, MeOH); ^{1}H NMR (400 MHz, D$_2$O): $\delta=1.31$ (m, 1H, *H*-5), 1.38–1.54 (m, 3H, 2*H*γ Arg, *H*β Arg), 1.60 (m, 1H, *H*-7), 1.78 (m, 1H, *H*-8), 1.98 (m, 1H, *H*β Arg), 2.28–2.43 (m, 3H, *H*-8, *H*-7, *H*-5), 2.57–2.69 (m, 2H, *H*-4, *H*β Asp), 3.00 (dd, 1H, $J=7.5$ Hz, $J=16.9$ Hz, *H*β Asp), 3.03–3.16 (m, 2H, 2*H*δ Arg), 3.42–3.50 (m, 3H, CH_2OH, *H*α Gly), 3.92 (m, 1H, *H*-6), 4.13–4.30 (m, 3H, *H*-9, *H*α Gly, *H*-3), 4.45 (t, 1H, $J=7.3$ Hz, *H*α Asp), 4.50 (dd, 1H, $J=3.9$ Hz, $J=10.6$ Hz, *H*α Arg); ^{13}C NMR HETCOR (400 MHz, D$_2$O): $\delta=62.0$, 61.0, 55.8, 52.32, 51.3, 51.2, 42.2, 40.3, 37.4, 33.2, 32.5, 31.6, 29.9, 26.7, 28.3, 24.1; for a more detailed NMR characterization, see the Supporting Information; MS (ESI$^+$) *m/z*: 539.2 $[M+H]^+$; Anal.: ($C_{22}H_{34}N_8O_8{\cdot}CF_3CO_2H$) C, H, N.

Compound 32. Yield: 30%; white foam; $[\alpha]_D^{22}=-75.60$ ($c=1.00$, MeOH); ^{1}H NMR (600 MHz, H_2O+D_2O): $\delta=1.43$–1.58 (m, 2H, 2*H*γ Arg) 1.62–1.70 (m, 2H, *H*-5, *H*-6), 1.70–1.88 (m, 5H, 2*H*β Arg, *H*-9, *H*-8, *H*-6), 1.94 (m, 1H, *H*-4), 2.03–2.16 (m, 2H, *H*-5, *H*-9), 2.20 (m, 1H, *H*-8), 2.73–2.80 (m, 2H, 2*H*β Asp), 3.05–3.20 (m, 2H, 2*H*δ Arg), 3.52 (m, 1H, HC*H*O), 3.56 (m, 1H, HC*H*O), 3.66 (dd, 1H, $J=14.3$ Hz, $J=6.4$ Hz, *H*α Gly), 3.73–3.88 (m, 2H, *H*α Gly, *H*-7), 4.12 (m, 1H, *H*-10), 4.18 (m, 1H, *H*α Arg), 4.42 (m, 1H, *H*-3), 4.74 (m, 1H, *H*α Asp), 7.09 (m, 1H, N*H* Arg), 7.36 (m, 1H, N*H* Asp), 7.59 (m, 1H, N*H* Temp), 8.82 (m, 1H, N*H* Gly); ^{13}C NMR HETCOR (600 MHz, H_2O+D_2O): $\delta=$ 65.6, 64.5, 59.8, 56.7, 53.4, 51.9, 44.3, 40.9, 40.4, 35.1, 33.0, 32.5, 30.8, 27.2, 26.0, 24.4; MS (ESI) *m/z*: 553.4 $[M+H]^+$; Anal.: ($C_{23}H_{36}N_8O_8{\cdot}CF_3CO_2H$) C, H, N.

Compound 33. Yield: 98%; white foam; $[\alpha]_D^{22}=-17.78$ ($c=1.05$, MeOH); ^{1}H NMR (400 MHz, D$_2$O): $\delta=1.44$–1.56 (m, 3H, 2*H*γ Arg, *H*-6), 1.56–1.69 (m, 2H, *H*β Arg, *H*-4), 1.73 (m, 1H, *H*-5), 1.78–1.93 (m, 3H, *H*-6, *H*-8, *H*-9), 1.93–2.07 (m, 2H, *H*-5, *H*β Arg), 2.20 (m, 1H, *H*-8), 2.39 (m, 1H, *H*-9), 2.72 (dd, 1H, $J=8.0$ Hz, $J=16.2$ Hz, *H*β Asp), 3.03 (dd, 1H, $J=8.0$ Hz, $J=16.2$ Hz, *H*β Asp), 3.08–3.23 (m, 2H, 2*H*δ Arg), 3.42–3.53 (m, 2H, *H*α Gly, HC*H*O), 3.58 (dd, 1H, $J=3.8$ Hz, $J=$ 11.4 Hz, HC*H*O), 4.20 (m, 1H, *H*-7), 4.24 (d, 1H, $J=12.0$ Hz, *H*α Gly), 4.40 (m, 1H, *H*-10), 4.46 (m, 1H, *H*α Arg), 4.55 (d, 1H, $J=12.0$ Hz, *H*-3), 4.64 (t, 1H, $J=7.2$ Hz, *H*α Asp); ^{13}C NMR HETCOR (400 MHz, D$_2$O): $\delta=63.9$, 63.5, 59.8, 53.0, 52.8, 51.0, 43.8, 41.0, 40.4, 34.0, 32.2, 30.1, 27.7, 27.5, 25.2; MS (ESI$^+$) *m/z*: 553.4 $[M+H]^+$; Anal.: ($C_{23}H_{36}N_8O_8{\cdot}CF_3CO_2H$) C, H, N.

Compound 42. Yield: 98%; white foam; $[\alpha]_D^{22}=-86.15$ ($c=0.4$, MeOH); ^{1}H NMR (400 MHz, D$_2$O): $\delta=0.84$ (t, 3H, $J=7.4$ Hz, $COCH_2CH_2CH_2CH_3$), 1.26 (m, 2H, $COCH_2CH_2CH_2CH_3$), 1.42 (m, 1H, *H*-5), 1.48–1.60 (m, 4H, 2*H*γ Arg, $COCH_2CH_2CH_2CH_3$), 1.64 (m, 1H, *H*β Arg), 1.72 (m, 1H, *H*-7), 1.82 (m, 1H, *H*β Arg), 1.95 (m, 1H, *H*-8), 2.10–2.30 (m, 5H, *H*-5, $COCH_2CH_2CH_2CH_3$, 1H, *H*-7, *H*-8), 2.36 (m, 1H, *H*-4), 2.71–2.86 (m, 2H, 2*H*β Asp), 3.03–3.31 (m, 4H, CH_2NHCO, 2*H*δ Arg), 3.24 (m, 1H, *H*CHNHCO), 3.56 (d, 1H, $J=14.3$ Hz, *H*α Gly), 3.66 (t, 1H, $J=10.4$ Hz, *H*-6), 4.04 (d, 1H, $J=14.3$ Hz, *H*α Gly), 4.26 (d, 1H, $J=10.1$ Hz, *H*-9), 4.3 (m, 1H, *H*α Arg), 4.63 (m, 1H, *H*α Asp), 4.74 (m, 1H, *H*-3); ^{13}C NMR HETCOR (100.6 MHz, D$_2$O): $\delta=$ 61.3, 59.9, 51.8, 51.7, 49.7, 44.5, 40.4, 39.8, 38.0, 36.9, 35.6, 30.8, 29.0, 28.9, 27.7, 27.3, 24.3, 21.5, 12.8; MS (ESI$^+$) *m/z*: 544.5 $[M+Na]^+$, 622.5 $[M+H]^+$; Anal.: ($C_{27}H_{43}N_9O_8{\cdot}CF_3CO_2H$) C, H, N.

Compound 43 Yield: 98%; white foam; $[\alpha]_D^{22}=-64.9$ ($c=0.68$, MeOH); ^{1}H NMR (400 MHz, D$_2$O): $\delta=0.83$ (t, 3H, $J=7.3$ Hz,

$COCH_2CH_2CH_2CH_3$), 1.14–1.30 (m, 3H, *H*-5, $COCH_2CH_2CH_2CH_3$), 1.40–1.54 (m, 4H, 2*H*γ Arg, $COCH_2CH_2CH_2CH_3$), 1.54–1.70 (m, 2H, *H*β Arg, *H*-7), 1.85 (m, 1H, *H*-8), 2.05 (m, 1H, *H*β Arg), 2.15 (t, 2H, *J*= 7.4 Hz, $COCH_2CH_2CH_2CH_3$), 2.35, 2.50 (m, 3H, *H*-8, *H*-7, *H*-5), 2.66–2.80 (m, 2H, *H*β Asp, *H*-4), 3.00–3.23 (m, 5H, *H*β Asp, 2*H*δ Arg, CH_2NHCO), 3.48 (d, 1H, *J*=14.6 Hz, *H*α Gly), 3.98 (m, 1H, *H*-6), 4.20–4.30 (m, 2H, *H*-9, *H*α Gly), 4.36 (t, 1H, *J*=7.0 Hz, *H*-3), 4.50 (t, 1H, *J*=7.2 Hz, *H*α Asp), 4.57 (dd, 1H, *J*=10.1 Hz, *J*=3.4 Hz, *H*α Arg); ^{13}C NMR (100.6 MHz, D_2O): δ=177.7, 174.8, 174.5, 174.0, 173.0, 171.6, 170.2, 62.1, 56.0, 52.9, 51.6, 51.3, 42.3, 40.3, 40.1, 35.8, 35.6, 33.2, 32.8, 32.6, 30.1, 27.5, 26.9, 24.3, 21.6, 13.0; MS (ESI^+) *m*/*z*: 622.3 $[M+H]^+$; Anal.: ($C_{27}H_{43}N_9O_8{\cdot}CF_3CO_2H$) C, H, N.

Compound 44. Yield: 98%; white solid; $[\alpha]_D^{22}=-12.6$ (*c*=1.00, MeOH); ^{1}H NMR (400 MHz, D_2O): δ=0.85 (t, 3H, *J*=7.3 Hz, $COCH_2CH_2CH_2CH_3$), 1.25 (m, 2H, $COCH_2CH_2CH_2CH_3$), 1.43–1.56 (m, 5H, $COCH_2CH_2CH_2CH_3$, 2*H*γ Arg, *H*-6), 1.56–1.69 (m, 2H, *H*β Arg, *H*-5), 1.75 (m, 1H, *H*-4), 1.73–2.04 (m, 5H, *H*-6, *H*-8, *H*-5, *H*β Arg, *H*-9), 2.12–2.27 (m, 3H, $COCH_2CH_2CH_2CH_3$, *H*-8), 2.4 (m, 1H, *H*-9), 2.73 (dd, 1H, *J*=17.0 Hz, *J*=6.7 Hz, *H*β Asp), 2.93–3.08 (m, 2H, *H*CHNHCO, *H*β Asp), 3.08–3.23 (m, 2H, 2*H*δ Arg), 3.42 (dd, 1H, *J*= 14.0 Hz, *J*=3.9 Hz, *H*CHNHCO), 3.47 (d, 1H, *J*=14.5 Hz, *H*α Gly), 4.17 (m, 1H, *H*-7), 4.22 (d, 1H, *J*=14.5 Hz, *H*α Gly), 4.39 (dd, 1H, *J*= 8.8 Hz, *J*=4.7 Hz, *H*-10), 4.46 (dd, 1H, *J*=10.6 Hz, *J*=4.2 Hz, *H*α Arg), 4.56 (m, 1H, *H*-3), 4.65 (dd, 1H, *J*=7.6 Hz, *H*α Asp); ^{13}C NMR HETCOR (400 MHz, D_2O): δ=62.8, 59.3, 55.2, 51.8, 50.6, 43.0, 41.4, 40.0, 38.1, 35.7, 33.2, 31.8, 31.7, 30.5, 27.4, 27.3, 27.0, 25.5, 21.4, 12.8; MS (ESI^+) *m*/*z*: 636.7 $[M+H]^+$; Anal.: ($C_{28}H_{45}N_9O_8{\cdot}CF_3CO_2H$) C, H, N.

Compound 45. Yield: 30%; white foam; $[\alpha]_D^{22}=-67.75$ (*c*=0.70, MeOH); ^{1}H NMR (600 MHz, H_2O+D_2O): δ=0.78 (t, 3H, *J*=7.5 Hz, $COCH_2CH_2CH_2CH_3$), 1.20 (m, 2H, $COCH_2CH_2CH_2CH_3$), 1.41–1.57 (m, 4H, 2*H*γ Arg, $COCH_2CH_2CH_2CH_3$) 1.66–1.85 (m, 6H, 2*H*β Arg, *H*-9, *H*-8, 2*H*-6), 1.89 (m, 1H, *H*-5), 2.02–2.13 (m, 2H, *H*-5, *H*-9), 2.15–2.24 (m, 2H, *H*-8, *H*-4), 2.27 (t, 2H, *J*=7.5 Hz, $COCH_2CH_2CH_2CH_3$), 2.72–2.83 (m, 2H, 2*H*β Asp), 3.06–3.17 (m, 2H, 2*H*δ Arg), 3.63 (m, 1H, *H*α Gly), 3.75–3.87 (m, 2H, *H*-7, *H*α Gly), 3.40 (dd, 1H, *J*=11.4 Hz, *J*=1.2 Hz, HC*H*O), 4.08 (m, 1H, *H*-10), 4.22 (m, 1H, *H*α Arg), 4.26 (m, 1H, HC*H*O), 4.50 (m, 1H, *H*-3), 4.61 (m, 1H, *H*α Asp), 7.09 (m, 1H, N*H* Arg), 7.26 (m, 1H, N*H* Asp), 7.62 (m, 1H, N*H* Temp), 8.83 (m, 1H, N*H* Gly); ^{13}C NMR HETCOR (600 MHz, H_2O+D_2O): δ=68.2, 65.8, 59.8, 56.0, 53.4, 51.4, 44.5, 40.5, 38.7, 34.7, 33.6, 33.3, 32.6, 31.9, 27.7, 26.5, 26.2, 24.6, 21.7, 13.0; MS (ESI) *m*/*z*: 636.5 $[M+H]^+$; Anal.: ($C_{28}H_{44}N_8O_9{\cdot}CF_3CO_2H$) C, H, N.

Solid-phase receptor binding assay

Purified $\alpha_v\beta_3$ and $\alpha_v\beta_5$ receptors (Chemicon International, Inc., Temecula, CA, USA) were diluted to 0.5 μg mL^{-1} in coating buffer containing 20 mM Tris-HCl (pH 7.4), 150 mM NaCl, 1 mM $MnCl_2$, 2 mM $CaCl_2$, and 1 mM $MgCl_2$. An aliquot of diluted receptors (100 μL well^{-1}) was added to 96-well microtiter plates (NUNC MW 96F Medisorp Straight) and incubated overnight at 4 °C. The plates were then incubated with blocking solution (coating buffer plus 1% bovine serum albumin) for an additional 2 h at room temperature to block nonspecific binding, followed by 3 h incubation at room temperature with various concentrations (10^{-10}–10^{-5} M) of test compounds in the presence of biotinylated vitronectin (1 μg mL^{-1}) using an EZ-Link Sulfo-NHS-Biotinylation kit (Pierce, Rockford, IL, USA). After washing, the plates were incubated for 1 h at room temperature with biotinylated streptavidin–peroxidase complex (Amersham Biosciences, Uppsala, Sweden) followed by 30 min incubation with 100 μL Substrate Reagent Solution (R&D Systems, Minneapolis, MN) before stopping the reaction with the addition of 50 μL 1 N H_2SO_4. Absorbance at 415 nm was read in a Synergy™ HT Multi-Detection Microplate Reader (BioTek Instruments, Inc.). Each data point represents the average of triplicate wells; data analysis was carried out by nonlinear regression analysis with GraphPad Prism software.

Cell cultures

Reagents were purchased from Sigma unless otherwise indicated. Human umbilical vein vascular endothelial cells (HUVEC) were obtained from Promocell GmbH (Heidelberg, Germany) and grown in medium M199 supplemented with 20% fetal calf serum (FCS), L-glutamine (2 mM), penicillin (100 U mL^{-1})/streptomycin (100 μg mL^{-1}), porcine heparin (100 μg mL^{-1}), and endothelial cell growth factor (ECGF; 50 ng mL^{-1}). HUVECs were maintained in culture and used at five passages. ECV-304 bladder carcinoma cells were kindly provided by Prof. M. L. Villa (University of Milan, Italy); despite their epithelial origin, ECV-304 cells share many characteristics with the human endothelium, and they are widely used as endothelial-like cells. ECV-304 cells were grown in medium M199 supplemented with 10% FCS, L-glutamine (2 mM), and penicillin (100 U mL^{-1})/streptomycin (100 μg mL^{-1}). Cells were maintained at 37 °C in an atmosphere of 95% air and 5% CO_2.

Cell adhesion assay

Plates (96 wells) were coated with fibronectin or vitronectin (Duotech) at 10 μg mL^{-1} in phosphate-buffered saline (PBS, Sigma) overnight at 4 °C. Cells (2.5×10^4 per 100 μL) were seeded in each well and allowed to adhere for 2 h at 37 °C in the presence of various concentrations of compound **31**. Nonadherent cells were removed with PBS. The remaining adherent cells were stained with a 0.5% solution of Crystal Violet for 10 min and rinsed with H_2O. Stained cells were solubilized with 1% SDS and quantified on a microtiter plate reader at 595 nm. Experiments were carried out in triplicate. Results are expressed as the mean compound concentration ±SE that inhibited 50% of cell adhesion (IC_{50}). The IC_{50} was calculated using GraphPad Prism 5 software.

Wound assay

Plates (24 wells) were coated with vitronectin (Duotech) at 10 μg mL^{-1} in PBS (Sigma) overnight at 4 °C. 1.6×10^5 HUVEC or ECV-304 cells were seeded and allowed to adhere overnight. Adherent cells were scratched with a p200 pipette tip, washed three times with M199, and immediately photographed with a Zeiss Axio Observer A1 inverted microscope equipped with a Zeiss AxioCam MRm. Subsequently, cells were incubated for 24 h (HUVEC) or 48 h (ECV-304) with 10 μM compound **31**, diluted in the basal medium of culture, and supplemented with 2% FCS. Control cells were scratched and cultured in the same medium without compound. After treatment, cells were photographed again to measure and compare wound healing. Images were printed on A4 paper, and the width of the wounds was evaluated and compared with a ruler, according to the experimental time course. Results are expressed as a percentage of closure relative to the width of the wound before treatment. Each point was done in triplicate, and the experiment was repeated twice.

Computational studies

All calculations were run using the Schrödinger suite of programs (http://www.schrodinger.com) through the Maestro graphical interface.

Conformational analysis. Conformational preferences of the RGD cyclopeptides were investigated by molecular mechanics calculations within the framework of MacroModel version 9.1,[29] using the MacroModel implementation of the Amber all-atom force field (denoted AMBER*) and the implicit water GB/SA solvation model of Still et al.[26,30] A two-step protocol was used. Monte Carlo/energy minimization (MC/EM) conformational searches of the AGA (Ala-Gly-Ala) cyclopeptide analogues containing methyl groups instead of the Arg and Asp side chains were performed as the first step.[22] Amide bonds were included among the rotatable bonds. For each search, at least 1000 starting structures for each variable torsion angle were generated and minimized until the gradient was < 0.05 kJ Å^{-1} mol^{-1} using the truncated Newton–Raphson method implemented in MacroModel.[31] Duplicate conformations and those with energy > 6 kcal mol^{-1} above the global minimum were discarded. Free simulations of the complete RGD cyclic peptides (Asp and Arg side chains were considered ionized) were then performed at 300 K using the metropolis Monte Carlo/stochastic dynamics (MC/SD) hybrid simulation algorithm,[25] starting from the cyclopeptide backbone geometries located by the previous MC/EM step. RGD side chain dihedral angles were defined as internal coordinate degrees of freedom in the Monte Carlo part of the algorithm. A time step of 1 fs was used for the stochastic dynamics part of the algorithm. At least two 10-ns simulations were run for each RGD cyclopeptide starting from different conformations to test the convergence. Samples were taken at 2-ps intervals during each simulation, yielding 5000 conformations for analysis.

Protein setup. The recently solved crystal structure of the extracellular domain of the integrin $\alpha_v\beta_3$ receptor in complex with EMD121974 and in the presence of the pro-adhesive ion Mn^{2+} (PDB code: 1L5G) was used for docking studies.[8] Docking was performed only on the globular head of integrin because the head group of integrin has been identified in the crystal structure as the ligand binding region. The protein structure was set up for docking as follows: the protein was truncated to residue sequences 41–342 for chain α and 114–347 for chain β. Due to a lack of parameters, the Mn^{2+} ions in the experimental protein structure were modeled by replacing them with Ca^{2+} ions. The charged protein groups that were neither located in the ligand binding pocket nor involved in salt bridges were neutralized by using the Schrödinger pprep script. The hydrogen atoms were added by using the Schrödinger graphical user interface Maestro, and the resulting structure was optimized using the Schrödinger impref script.

Docking. The automated docking calculations were performed using Glide (Grid-based Ligand Docking with Energetics) within the framework of Impact version 4.5.[27] Glide uses a hierarchical series of filters to search for possible locations of the ligand in the active site region of the receptor. The shape and properties of the receptor are represented on a grid by several different sets of fields that provide progressively more accurate scoring of the ligand poses. To begin the Glide calculation, an enclosing box and a bounding box are defined starting from the center of the reference ligand. The starting poses for the ligands to be screened are generated by placing the center of the ligand in random points of the bounding box. Conformational flexibility is handled in Glide by an extensive conformational search, augmented by a heuristic screen that rapidly eliminates conformations deemed unsuitable for binding to a receptor, such as conformations that have long-range internal hydrogen bonds. After all the filters have been applied, the remaining best 400 poses are partially minimized in the grid field using OPLSAA and finally scored using the GlideScore scoring function. GlideScore is based on ChemScore,[32] but includes a steric clash term and adds buried polar terms to penalize electrostatic mismatches. The grid-generation step started from the extracellular fragment of the crystal structure of $\alpha_v\beta_3$ in complex with EMD121974, as described in the protein setup section, and used mae input files of both ligand and active site, including hydrogen atoms. The center of the grid enclosing box was defined by the center of the bound ligand, as described in the original PDB entry. The enclosing box dimensions, which are automatically deduced from the ligand size, fit the entire active site. For the docking step, the size of the bounding box for placing the ligand center was set to 12 Å. No further modifications were applied to the default settings. The GlideScore function was used to select 30 poses for each ligand. The Glide program was initially tested for its ability to reproduce the crystallized binding geometry of EMD121974. The program was successful in reproducing the experimentally determined binding mode of this compound, as it corresponds to the best-scored pose.

NMR spectroscopy

NMR experiments were performed at a temperature of 294 K on Bruker Avance 400 and 600 MHz spectrometers. All proton and carbon chemical shifts were assigned unambiguously. The NMR experiments were carried out in a D_2O/H_2O 1:9 mixture in order to observe amide protons. Two-dimensional experiments (TOCSY, COSY, NOESY, and HSQC) were carried out on samples of **30** and **31** at a concentration of 3 mM. NOESY experiments were performed at 0.2, 0.4, 0.6 and 0.8 s. The water resonance was saturated with the excitation sculpting sequence from the Bruker library. The conformation of the pentapeptide was first analyzed with respect to hydrogen bonding of amide protons (VT-NMR spectroscopy) and NOE contacts.

Acknowledgements

The authors thank CNR and MUR (FIRB RBNE03 LF7X and PRIN 2006030449 research projects) for financial support and CILEA for computing facilities. E.M.V.A. was supported by a fellowship from the Doctorate School of Molecular Medicine, University of Milan.

Keywords: azabicycloalkanes · inhibitors · integrins · peptidomimetics · RGD motif

[1] a) J. Folkman, *Nat. Med.* **1995**, *1*, 27–31; b) S. A. Mousa, *Drugs Future* **1998**, *23*, 51–60; c) S. A Mousa, *Emerging Ther. Targets* **2000**, *4*, 143–153; d) P. Carmeliet, *Nat. Med.* **2000**, *6*, 389–395; e) O. Bögler, T. Mikkelsen, *Cancer J.* **2003**, *9*, 205–213; f) J. Folkman, *Semin. Oncol.* **2002**, *29*, 15–18; g) R. Hwang, J. V. Varner, *Hematol. Oncol. Clin. North Am.* **2004**, *18*, 991–1006.

[2] a) J. D. Hood, D. A. Cheresh, *Nat. Rev. Cancer* **2002**, *2*, 91–100; b) R. O. Hynes, *Cell* **2002**, *110*, 673–687.

[3] a) E. Ruoslahti, M. D. Pierschbacher, *Cell* **1986**, *44*, 517–518; b) S. E. Souza, M. H. Ginsberg, E. F. Plow, *Trends Biochem. Sci.* **1991**, *16*, 246–250.

[4] a) E. F. Plow, T. A. Haas, L. Zhang, J. Loftus, J. W. Smith, *J. Biol. Chem.* **2000**, *275*, 21785–21788; b) K. Suehiro, J. W. Smith, E. F. Plow, *J. Biol. Chem.* **1996**, *271*, 10365–10371.

[5] a) E. Noiri, J. Gailit, D. Sheth, H. Magazine, M. Gurrath, G. Müller, H. Kessler, M. S. Goligorsky, *Kidney Int.* **1994**, *46*, 1050–1058; b) M. Friedlander, C. L. Theesfeld, M. Sugita, M. Fruttiger, M. A. Thomas, S. Chang, D. A. Cheresh, *Proc. Natl. Acad. Sci. USA* **1996**, *93*, 9764–9769; c) Z. Yun, D. G. Menter, G. L. Nicolson, *Cancer Res.* **1996**, *56*, 3103–3111; d) D. K. Kaul, H. M. Tsai, X. D. Liu, M. T. Nakada, R. L. Nagel, B. S. Coller, *Blood* **2000**, *95*, 368–374.

[6] a) P. C. Brooks, R. A. Clark, D. A. Cheresh, *Science* **1994**, *264*, 569–571; b) M. E. Duggan, J. H. Hutchinson, *Exp. Opin. Ther. Pat.* **2000**, *10*, 1367–1383.
[7] M. Friedlander, P. C. Brooks, R. W. Shaffer, C. M. Kincaid, J. A. Varner, D. A. Cheresh, *Science* **1995**, *270*, 1500–1502.
[8] a) J.-P. Xiong, T. Stehle, B. Diefenbach, R. Zhang, R. Dunker, D. L. Scott, A. Joachimiak, S. L. Goodman, M. A. Arnaout, *Science* **2001**, *294*, 339–345; b) J.-P. Xiong, T. Stehle, R. Zhang, A. Joachimiak, M. Frech, S. L. Goodman, M. A. Arnaout, *Science* **2002**, *296*, 151–155.
[9] a) R. Haubner, D. Finsinger, H. Kessler, *Angew. Chem.* **1997**, *109*, 1440–1456; *Angew. Chem. Int. Ed. Engl.* **1997**, *36*, 1374–1389; b) A. C. Bach, J. R. Espina, S. A. Jackson, P. F. Stouten, J. L. Duke, S. A. Mousa, W. F. DeGrado, *J. Am. Chem. Soc.* **1996**, *118*, 293–294; c) G. Müller, M. Gurrath, H. Kessler, *J. Comput. Aided Mol. Des.* **1994**, *8*, 709–730; d) R. M. Scarborough, M. A. Naughton, W. Teng, J. W. Rose, D. R. Phillips, L. Nannizzi, A. Arfsten, A. M. Campbell, I. F. Charo, *J. Biol. Chem.* **1993**, *268*, 1066–1073.
[10] R. Haubner, R. Gratias, B. Diefenbach, S. L. Goodman, A. Jonczyk, H. Kessler, *J. Am. Chem. Soc.* **1996**, *118*, 7461–7472.
[11] a) E. Lohof, E. Planker, C. Mang, F. Burkhart, M. A. Dechantsreiter, R. Haubner, H.-J. Wester, M. Schwaiger, G. Hölzemann, S. L. Goodman, H. Kessler, *Angew. Chem.* **2000**, *112*, 2868–2871; *Angew. Chem. Int. Ed.* **2000**, *39*, 2761–2764; b) F. Schumann, A. Müller, M. Koksch, G. Müller, N. Sewald, *J. Am. Chem. Soc.* **2000**, *122*, 12009–12010; c) R. Haubner, W. Schmitt, G. Hölzemann, S. L. Goodman, A. Jonczyk, H. Kessler, *J. Am. Chem. Soc.* **1996**, *118*, 7881–7891.
[12] M. A. Dechantsreiter, E. Planker, B. Mathä, E. Lohof, G. Hölzemann, A. Jonczyk, S. L. Goodman, H. Kessler, *J. Med. Chem.* **1999**, *42*, 3033–3040.
[13] H. N. Lode, T. Moehler, R. Xiang, A. Jonczyk, S. D. Gillies, D. A. Cheresh, R. A. Reisfeld, *Proc. Natl. Acad. Sci. USA* **1999**, *96*, 1591–1596.
[14] a) G. Casiraghi, G. Rassu, L. Auzzas, P. Burreddu, E. Gaetani, L. Battistini, F. Zanardi, C. Curti, G. Nicastro, L. Belvisi, I. Motto, M. Castorina, G. Giannini, C. Pisano, *J. Med. Chem.* **2005**, *48*, 7675–7687; b) F. Zanardi, P. Burreddu, G. Rassu, L. Auzzas, L. Battistini, C. Curti, A. Sartori, G. Nicastro, G. Menchi, N. Cini, A. Bottonocetti, S. Raspanti, G. Casiraghi, *J. Med. Chem.* **2008**, *51*, 1771–1782.
[15] a) M. Angiolini, S. Araneo, L. Belvisi, E. Cesarotti, A. Checchia, L. Crippa, L. Manzoni, C. Scolastico, *Eur. J. Org. Chem.* **2000**, *14*, 2571–2581; b) L. Belvisi, A. Bernardi, L. Manzoni, D. Potenza, C. Scolastico, *Eur. J. Org. Chem.* **2000**, *14*, 2563–2569.
[16] a) L. Belvisi, A. Bernardi, A. Checchia, L. Manzoni, D. Potenza, C. Scolastico, M. Castorina, A. Cupelli, G. Giannini, P. Carminati, C. Pisano, *Org. Lett.* **2001**, *3*, 1001–1004; b) L. Belvisi, T. Riccioni, M. Marcellini, L. Vesci, I. Chiarucci, D. Efrati, D. Potenza, C. Scolastico, L. Manzoni, K. Lombardo, M. A. Stasi, A. Orlandi, A. Ciucci, B. Nico, D. Ribatti, G. Giannini, M. Presta, P. Carminati, C. Pisano, *Mol. Cancer Ther.* **2005**, *4*, 1670–1680.
[17] a) E. Artale, G. Banfi, L. Belvisi, L. Colombo, M. Colombo, L. Manzoni, C. Scolastico, *Tetrahedron* **2003**, *59*, 6241–6250; b) A. Bracci, L. Manzoni, C. Scolastico, *Synthesis* **2003**, 2363–2367; c) F. M. Bravin, G. Busnelli, M. Colombo, F. Gatti, L. Manzoni, C. Scolastico, *Synthesis* **2004**, 353–358; d) L. Manzoni, L. Belvisi, M. Colombo, E. Di Carlo, A. Forni, C. Scolastico, *Tetrahedron Lett.* **2004**, *45*, 6311–6315.
[18] L. Manzoni, D. Arosio, L. Belvisi, A. Bracci, M. Colombo, D. Invernizzi, C. Scolastico, *J. Org. Chem.* **2005**, *70*, 4124–4132.
[19] D. Arosio, L. Belvisi, L. Colombo, M. Colombo, D. Invernizzi, L. Manzoni, D. Potenza, M. Serra, M. Castorina, C. Pisano, C. Scolastico, *ChemMedChem* **2008**, *3*, 1589–1603.
[20] Further investigations to fully characterize this byproduct and to understand the mechanism of the side reaction are in progress, and will be reported in due course.
[21] G. Serini, D. Valdembri, F. Bussolino, *Exp. Cell Res.* **2006**, *312*, 651–658.
[22] G. Chang, W. C. Guida, W. C. Still, *J. Am. Chem. Soc.* **1989**, *111*, 4379–4386.
[23] L. Belvisi, A. Bernardi, M. Colombo, L. Manzoni, D. Potenza, C. Scolastico, G. Giannini, M. Marcellini, T. Riccioni, M. Castorina, P. LoGiudice, C. Pisano, *Bioorg. Med. Chem.* **2006**, *14*, 169–180.
[24] G. D. Rose, L. M. Gierasch, J. A. Smith, *Adv. Protein Chem.* **1985**, *37*, 1–109.
[25] F. Guarnieri, W. C. Still, *J. Comput. Chem.* **1994**, *15*, 1302–1310.
[26] W. C. Still, A. Tempczyk, R. C. Hawley, T. Hendrickson, *J. Am. Chem. Soc.* **1990**, *112*, 6127–6129.
[27] Glide version 4.5, Schrödinger LLC, New York, NY (USA).
[28] D. Potenza, L. Belvisi, *Org. Biomol. Chem.* **2008**, *6*, 258–262.
[29] MacroModel version 9.1, Schrödinger LLC, New York, NY (USA).
[30] S. J. Weiner, P. A. Kollman, D. T. Nguyen, D. A. Case, *J. Comput. Chem.* **1986**, *7*, 230–252.
[31] J. W. Ponder, F. M. Richards, *J. Comput. Chem.* **1987**, *8*, 1016–1024.
[32] M. D. Eldridge, C. W. Murray, T. R. Auton, G. V. Paolini, R. P. Mee, *J. Comput. Aided Mol. Des.* **1997**, *11*, 425–445.

Received: December 9, 2008
Revised: January 9, 2009
Published online on February 11, 2009

